Integrated stratigraphic, geochemical, and paleontological late Ediacaran to early Cambrian records from southwestern Mongolia

Emily F. Smith†, Francis A. Macdonald, Tanya A. Petach, Uyanga Bold, and Daniel P. Schrag
Department of Earth and Planetary Sciences, Harvard University, Cambridge, Massachusetts 02138, USA

ABSTRACT

The Zavkhan terrane in western Mongolia preserves thick, fossiliferous, carbonate-rich strata that span the Ediacaran-Cambrian transition. Measured stratigraphic sections and geological mapping of these strata, which include the Zuun-Arts, Bayangol, Salaagol, and Khairkhan Formations, reveal large lateral facies changes over short distances that necessitate revisions to previous lithostratigraphic correlations and biostratigraphic range charts. Here, we integrate new geological mapping and measured stratigraphic sections across the Zavkhan terrane with high-resolution carbon isotope ($\delta^{13}C$) chemostratigraphy, sequence stratigraphy, and biostratigraphy. Using these data, we revise correlations within the Zavkhan terrane and place small shelly fossil and ichnofossil horizons in a refined temporal and spatial framework. Finally, we integrate these data from Mongolia with absolute ages and chemostratigraphy from sections in Morocco and Oman. Our revised age model suggests that deposition of the Bayangol Formation and the lower part of the Salaagol Formation was limited to the Nemakit-Daldynian and Tommotian Stages.

With the new correlations and age model, we place the small shelly fossil first appearance datum in the basal Bayangol Formation instead of the basal Zuun-Arts Formation, which moves this horizon hundreds of meters higher in the stratigraphy, above the large negative excursion in the Zuun-Arts Formation. The first appearance datum of *Treptichnus pedum* is ~275 m above the large negative excursion in the Zuun-Arts Formation and ~250 m above the first appearance datum of small shelly fossils, highlighting the rarity and facies dependence of its preservation.

We shift the first appearance datums of tommotiids, orthothecimorphs, hyolithelminths, cap-shaped fossils, protoconodonts, and *Salanacus* to just below the positive peak 3p. This interpretation differs from previous chronostratigraphic placements of first appearance data of genera between positive excursions 1p and 2p. Using this level as the first appearance datum in Mongolia for these genera, we replot global fossil first appearances. With this new compilation, there are still three distinct pulses of fossil first appearances, as was suggested in previous compilations; however, we suggest that this pattern is controlled largely by regional sedimentation and taphonomy rather than the rate of taxonomic origination.

INTRODUCTION

Since Charles Darwin's observation of the apparently rapid appearance of fossils in what is now known as Cambrian strata (Darwin, 1859), the Precambrian-Cambrian boundary has been widely regarded as one of the evolutionary pivot points in the history of life. Despite the persisting interest on this topic, the causes, triggers, and tempo of change remain controversial. Following the extinction of Ediacaran biota and the calcifying metazoan *Cloudina*, the early Cambrian (or Terreneuvian Series) encompasses an evolutionary interval characterized by increases in diversity and disparity (Marshall, 2006) that coincide with multiple carbon isotope excursions with amplitudes of <8‰ (e.g., Zhu et al., 2006; Porter, 2007; Maloof et al., 2010a; Erwin et al., 2011) over a geologically brief interval in Earth history (Valentine, 2002). Most recently, Maloof et al. (2010a) suggested that the Cambrian fossil first appearances occurred in three discrete pulses associated with rapid reorganizations in the carbon cycle. To test this hypothesis and others about mechanistic links between environmental change and evolutionary milestones across the Ediacaran-Cambrian transition, it is necessary to integrate records around the globe. However, previous global syntheses (e.g., Maloof et al., 2010a) have been limited to a small number of localities with large uncertainties in both local and global stratigraphic correlations and the lack of absolute ages directly linked to biostratigraphic and chemostratigraphic data, particularly with respect to critical data from Asia. Because the global data set is biased by just a few localities, refining local correlations and grounding them in regional geology are necessary before an accurate global synthesis of fossil occurrence data can be constructed and interpreted.

The Ediacaran-Cambrian boundary is defined at the global bondary stratotype section and point (GSSP) as the first appearance datum (FAD) of the bilaterian trace fossil *Treptichnus pedum* (Landing, 1994), but the boundary has also been associated with the FAD of small shelly fossils and a large negative carbon isotope excursion (Narbonne et al., 1994; Corsetti and Hagadorn, 2000). These occurrences in the rock record are generally assumed to be broadly coincident, but both the precise and relative timing of these evolutionary milestones and perturbations to the carbon cycle are not directly constrained. The subsequent earliest Cambrian period is marked by FADs of small shelly fossils in many clades and high-frequency oscillations in the carbon cycle (Maloof et al., 2010a), but again, there are few absolute ages tied to these FADs or excursions. Because there is no one section globally in which it is possible to integrate the ichnofossil record, body fossil record, carbon isotope chemostratigraphy, and absolute ages, the calibration of this evolutionarily important transition remains piecemeal, resulting in much uncertainty in determining rates of origination and geochemical change. With a dearth of absolute ages tied to the fossil record, carbon isotope ($\delta^{13}C$) chemostratigraphy has proven to be a powerful tool for global correlation of Ediacaran-Cambrian successions (Brasier et al., 1990, 1993; Kirschvink et al., 1991; Knoll et al., 1995a; Zhu et al., 2006, 2007; Maloof et al., 2010b).

The Zavkhan (Dzabkhan) terrane in western Mongolia hosts thick, well-exposed, low-grade,

†E-mail: efsmith@fas.harvard.edu

GSA Bulletin; March/April 2016; v. 128; no. 3/4; p. 442–468; doi: 10.1130/B31248.1; 13 figures; 1 table; Data Repository item 2015265; published online 2 September 2015.

carbonate-rich, fossiliferous successions of late Ediacaran through early Cambrian strata, providing an opportunity to more precisely calibrate evolutionary changes in a chemo- and sequence-stratigraphic context. This succession hosts dozens of well-exposed sections with several horizons of small shelly fossils, archaeocyathid reefs, and ichnofossils (Goldring and Jensen, 1996; Khomentovsky and Gibsher, 1996; Kruse et al., 1996), many of which are being reported and documented here for the first time. However, because Ediacaran to early Cambrian strata in the Zavkhan terrane were deposited in a foreland basin (Macdonald et al., 2009), topography generated during tectonism resulted in large lateral facies changes, which confounded previous lithostratigraphic correlations and biostratigraphic compilations (Brasier et al., 1996b; Khomentovsky and Gibsher, 1996). In this study, we present new geological mapping and small shelly fossil biostratigraphy for the Nemakit-Daldynian through Tommotian strata in the necessary context of a high-resolution $\delta^{13}C$ chemostratigraphic age model and basinwide sequence stratigraphy.

Because there are only a handful of carbonate-rich fossiliferous sections globally that span the Ediacaran-Cambrian transition, namely, sections in Siberia, China, Kazakhstan, SW United States, NW Canada, and Mongolia, calibrating the timing and tempo of the radiation is heavily influenced by each record. This contribution of an age model, geological mapping, and revised biostratigraphy change known global rates of early Cambrian evolution and provide the necessary geological and stratigraphic framework for integrating geochemical, paleontological, and geochronological data from southwest Mongolia into the global record of the Ediacaran-Cambrian transition.

GEOLOGIC BACKGROUND AND TECTONOSTRATIGRAPHIC FRAMEWORK

Previous Studies

The Zavkhan terrane is a Precambrian crustal fragment embedded in the core of the Central Asian orogenic belt (Fig. 1). After late Ediacaran to Ordovician accretion of arc terranes to the south, the Late Ordovician to Silurian record of Mongolia is marked by extensional magmatism and basin formation (Kröner et al., 2010; Gibson et al., 2013). During this time, the Zavkhan terrane was part of a composite ribbon continent that was adjacent to Siberia (Wilhem et al., 2012). From the Devonian to Early Permian, the Zavkhan terrane was oroclinally buckled during the arrival of North China and Tarim (Lehmann et al., 2010; Edel et al., 2014). Locally, on the Zavkhan terrane, this late Paleozoic collision is manifested in dextral strike-slip wrench structures (Figs. 1A and 1C) and widespread Permian plutonism (Jahn et al., 2009).

The Neoproterozoic through Cambrian stratigraphy of the Zavkhan terrane was first described by Bezzubtsev (1963) in the Bayan Gorge. Before the early 1990s, research in Mongolia was largely restricted to Mongolian and Russian researchers who worked primarily on the Ediacaran through early Cambrian strata in the Zavkhan terrane (Zhegallo and Zhuravlev, 1991). Shortly after Mongolia opened back up to Western researchers, an international research team participated in International Geoscience Programme (IGCP) Project 303, "Precambrian-Cambrian Event Stratigraphy," in 1993, representing the first effort to bring together specialists from different subdisciplines of earth sciences for an integrated approach to addressing the Precambrian-Cambrian transition in western Mongolia. During this international excursion, they visited five previously documented sections to study them in more detail. The *Geological Magazine* publications that resulted from this project were the first time these key sections were described in English and placed into a regional and global context (Brasier et al., 1996a, 1996b; Goldring and Jensen, 1996; Khomentovsky and Gibsher, 1996; Kruse et al., 1996; Lindsay et al., 1996a, 1996b).

Voronin et al. (1982), Gibsher and Khomentovsky (1990), Gibsher et al. (1991), and Khomentovsky and Gibsher (1996) described the stratigraphy and published preliminary, schematic, hand-drawn maps of the southern and northern blocks of the Bayan Gorge, Tsagaan Gorge, Salaa Gorge, and Taishir. In addition, biostratigraphy is documented from Orolgo (Orolchayan) Gorge (Endonzhamts and Lkhasuren, 1988) and Kvetee Tsakhir Nuruu (Zhegallo and Zhuravlev, 1991; Dorjnamjaa et al., 1993; Esakova and Zhegallo, 1996). Detailed paleontological work was conducted primarily by Russian paleontologists; however, much of this work lacked a stratigraphic context. The series of 1996 publications was the first attempt at placing the small shelly fossil first appearances in a lithostratigraphic and chemostratigraphic framework (Brasier et al., 1996b; Khomentovsky and Gibsher, 1996). Brasier et al. (1996b) presented the first carbon, oxygen, and strontium chemostratigraphy for the Neoproterozoic through Cambrian carbonates in the Zavkhan terrane. More recently, the age and depositional environment of the Cryogenian strata have been more tightly constrained by Macdonald et al. (2009), Macdonald (2011), and Bold et al. (2013).

Cryogenian to Early Ediacaran Stratigraphy

Along the Zavkhan River, the oldest exposed rocks are felsic volcanic rocks of the Zavkhan Formation (Figs. 1B and 1C; Bold et al., 2013), which have been dated using laser ablation inductively coupled plasma mass spectrometry (LA-ICP-MS) U/Pb dating on zircon to between 773.5 ± 3.6 and 803.4 ± 8.0 Ma (Levashova et al., 2010). Granites that intrude the Zavkhan Formation have been dated using thermal ionization mass spectrometry (TIMS) bulk multigrain U/Pb on zircon at 755 ± 3 Ma (Yarmolyuk et al., 2008). The Zavkhan Formation is overlain by the synrift siliciclastic deposits informally referred to as the Khasagt Suite (Ruzhentsev and Burashnikov, 1996) and passive-margin deposits of the Tsagaan-Olom Group (Macdonald et al., 2009; Bold et al., 2013).

The Tsagaan-Olom Group (note recent changes in spelling and formalization of stratigraphy; Bold et al., 2013) contains two Cryogenian glacial diamictites and cap carbonates (Macdonald et al., 2009). The oldest formation in this group is the Maikhan-Uul Formation, a Sturtian-aged diamictite (Lindsay et al., 1996b; Macdonald et al., 2009; Macdonald, 2011), which has been constrained globally by correlation to between ca. 717 and 660 Ma (Macdonald et al., 2010; Rooney et al., 2014). Overlying the Maikhan-Uul Formation, there is the carbonate-dominated Taishir Formation, composed of the Sturtian cap carbonate and interglacial strata (Shields et al., 2002; Macdonald et al., 2009; Macdonald, 2011; Johnston et al., 2012; Shields-Zhou et al., 2012). The overlying Khongor and Ol Formations have been correlated to Marinoan glacial deposits and the ca. 635 Ma basal Ediacaran cap carbonate, respectively (Condon et al., 2005; Macdonald et al., 2009; Calver et al., 2013). The Ol Formation is overlain by the early Ediacaran Shuurgat Formation (previously referred to informally as the Ulaan Bulaagyn member of the Tsagaan-Olom Formation), which consists of 100–500 m of carbonate and is unconformably overlain by the latest Ediacaran Zuun-Arts Formation (Macdonald et al., 2009; Bold et al., 2013).

Latest Ediacaran to Early Cambrian Stratigraphy, Biostratigraphy, and Chemostratigraphy

During the latest Ediacaran, the Zavkhan terrane began to subduct to the southwest beneath the Khantaishir-Dariv arc, creating the foreland basin that accommodated the subsequent thick sequence of latest Ediacaran to earliest Cambrian strata (Macdonald et al., 2009). These

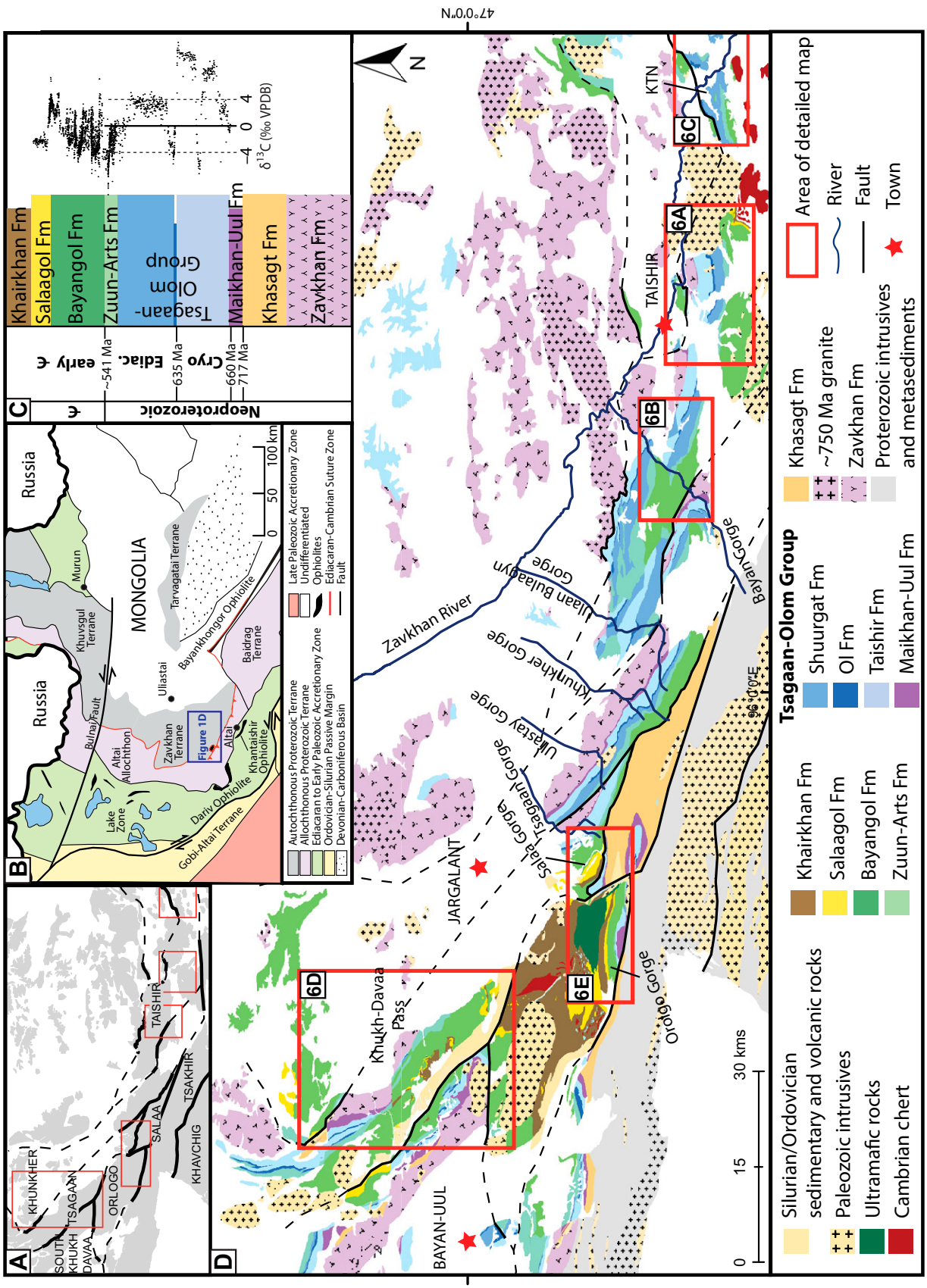

Figure 1. (A) Shaded outcrop of Zavkhan terrane showing major fault blocks. (B) Terrane map of Mongolia. Area of Figure 1D is boxed in dark blue. Map is adapted from Bucholz et al. (2014). (C) $\delta^{13}C$ profile from Macdonald et al. (2009) and this study plotted against generalized early Cambrian through Neoproterozoic stratigraphy in the Zavkhan terrane. The age constraints are dated by correlation. The basal Maikhan-Uul Formation has been correlated with the basal Sturtian glacial deposit in NW Canada at 717.4 ± 0.2 Ma (Macdonald et al., 2010) and 662.4 ± 3.9 Ma (Rooney et al., 2014). The Ol cap carbonate has been correlated with the Marinoan cap, which has been dated globally at ca. 635 Ma (Calver et al., 2004, 2013; Condon et al., 2005). VPDB—Vienna Peedee belemnite. (D) Geologic map of the Zavkhan terrane. Red boxes mark spatial extent of detailed maps in Figure 6. KTN—Kvetee Tsakhir Nuruu.

strata, along with kilometers of Neoproterozoic strata, are exposed in NE-vergent thrust sheets in the Zavkhan terrane.

From oldest to youngest, the late Ediacaran and early Cambrian strata on the Zavkhan terrane are the carbonate-dominated Zuun-Arts Formation, the mixed carbonate-siliciclastic Bayangol Formation, the carbonate-dominated Salaagol Formation, and the siliciclastic Khairkhan Formation (Fig. 2). Together, these strata range from ~800 to 2700 m in thickness. The Khairkhan Formation consists of allochthonous mélange, flysch, and molasse, marking the closure of the foredeep and the end of deposition in this basin (Macdonald et al., 2009).

Zuun-Arts Formation

Strata above the uppermost karst surface in the underlying Shuurgat Formation are marked by buff- to pink-colored microbial dolostone that preserves the columnar stromatolite *Boxonia grumulosa* (Fig. 3A; Markova et al., 1972). The distinct stromatolitic horizon is overlain by variably phosphatized green shale with nodular carbonate, marking an abrupt flooding surface. In some localities, a lag deposit of coarse, immature sandstone is present between the stromatolite and phosphatic shale. Overlying the phosphatic shale, there is ~150–400 m of thinly bedded, medium-gray limestone (Fig. 3B) with occasional intraclast breccia. The top 5–200 m section of the Zuun-Arts Formation consists of several 5–20-m-scale parasequences culminating with a distinctive white and black cross-bedded ooid grainstone (Fig. 3C). The top contact of the Zuun-Arts Formation is defined at a sharp contact between the ooid grainstone and a second horizon of microcrystalline phosphatic shale (Fig. 3D; Lindsay et al., 1996a).

The FAD of anabaritids, the earliest small shelly fossil, has been reported near the base of the Zuun-Arts Formation (Endonzhamts and Lkhasuren, 1988; Dorjnamjaa et al., 1993; Brasier et al., 1996b; Khomentovsky and Gibsher, 1996); however, we refine the position of this FAD horizon herein. Simple bed planar trace fossils are also present in this formation (Brasier et al., 1996b). Neither cloudinid nor the Shuram carbon isotope excursion has been documented in the Zuun-Arts or Shuurgat Formations. Carbon isotope ($\delta^{13}C$) values of the Shuurgat Formation range between –0.5‰ and +8.5‰, values that more closely resemble the carbon isotopic profile of the lower Ediacaran than the upper Ediacaran (Macdonald et al., 2009), which would imply a substantial hiatus at the karst surface between the Shuurgat and Zuun-Arts Formations (Macdonald et al., 2009; Bold et al., 2013).

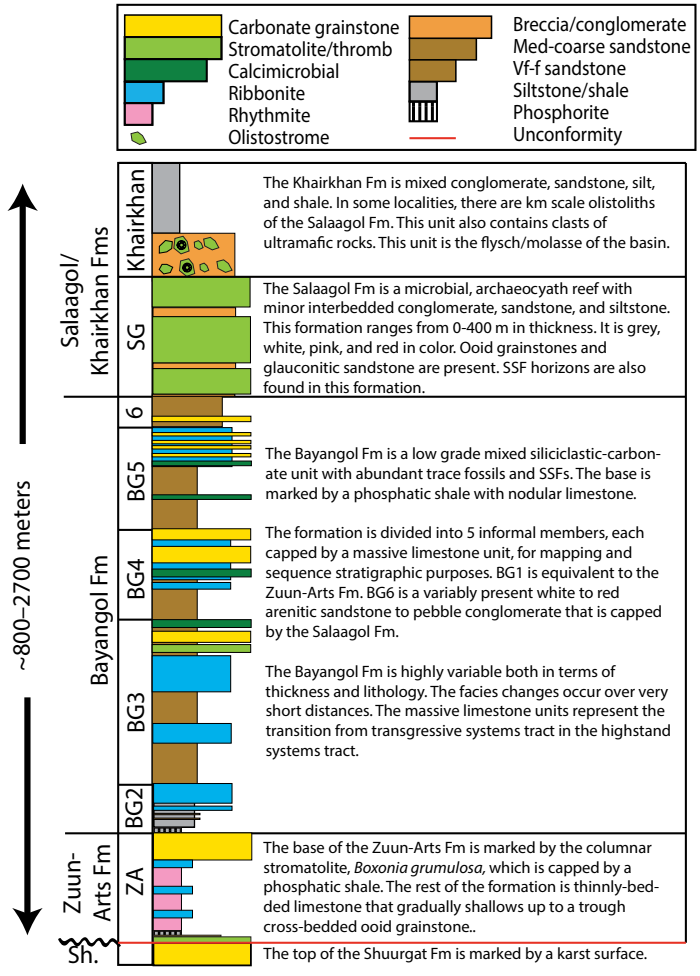

Figure 2. Generalized late Ediacaran to early Cambrian stratigraphy of the Zavkhan terrane. Note the recent changes in spelling and formalization of stratigraphy in the Zavkhan terrane by Bold et al. (2013). SSF—Small shelly fossils.

Bayangol Formation

The Bayangol Formation, along with the underlying Zuun-Arts and Shuurgat Formations, was previously included in the Tsagaan-Olom Formation and has been characterized and subdivided as numbered units by Voronin et al. (1982), Gibsher and Khomentovsky (1990), and Gibsher et al. (1991). The base of the Bayangol Formation is marked by phosphatic shale with nodular carbonate. The Bayangol Formation consists of mixed carbonate and siliciclastic strata, and it ranges from ~500 to 1250 m in thickness. In most sections in the basin, in the lower to middle part of the formation, there are at least three thick limestone units capping interbedded siliciclastic and limestone units. Figure 4 shows examples of a few of these massive limestone units and how they mark some of the large-scale sequence boundaries in the strata. In most sections in the basin, above the massive third limestone marker bed, there are hundreds of meters of predominantly fine to coarse sandstone.

The Bayangol Formation hosts diverse and well-preserved stromatolites, thrombolites, and other bioconstructions with a wide range in size and morphology (Kruse et al., 1996). Important for this study, there is also a rich assemblage of small shelly fossil and abundant trace fossils that have been previously documented in the Bayan, Salaa, and Tsagaan Gorges, Taishir, and Kvetee Tsakhir Nuruu (Fig. 1; Korobov and Missarzhevsky, 1977; Voronin et al., 1982; Endonzhamts and Lkhasuren, 1988; Goldring and Jensen, 1996; Khomentovsky and Gibsher, 1996). To create a composite biostratigraphic range chart for the Bayangol Formation, these sections were previously correlated primarily using lithostrati-

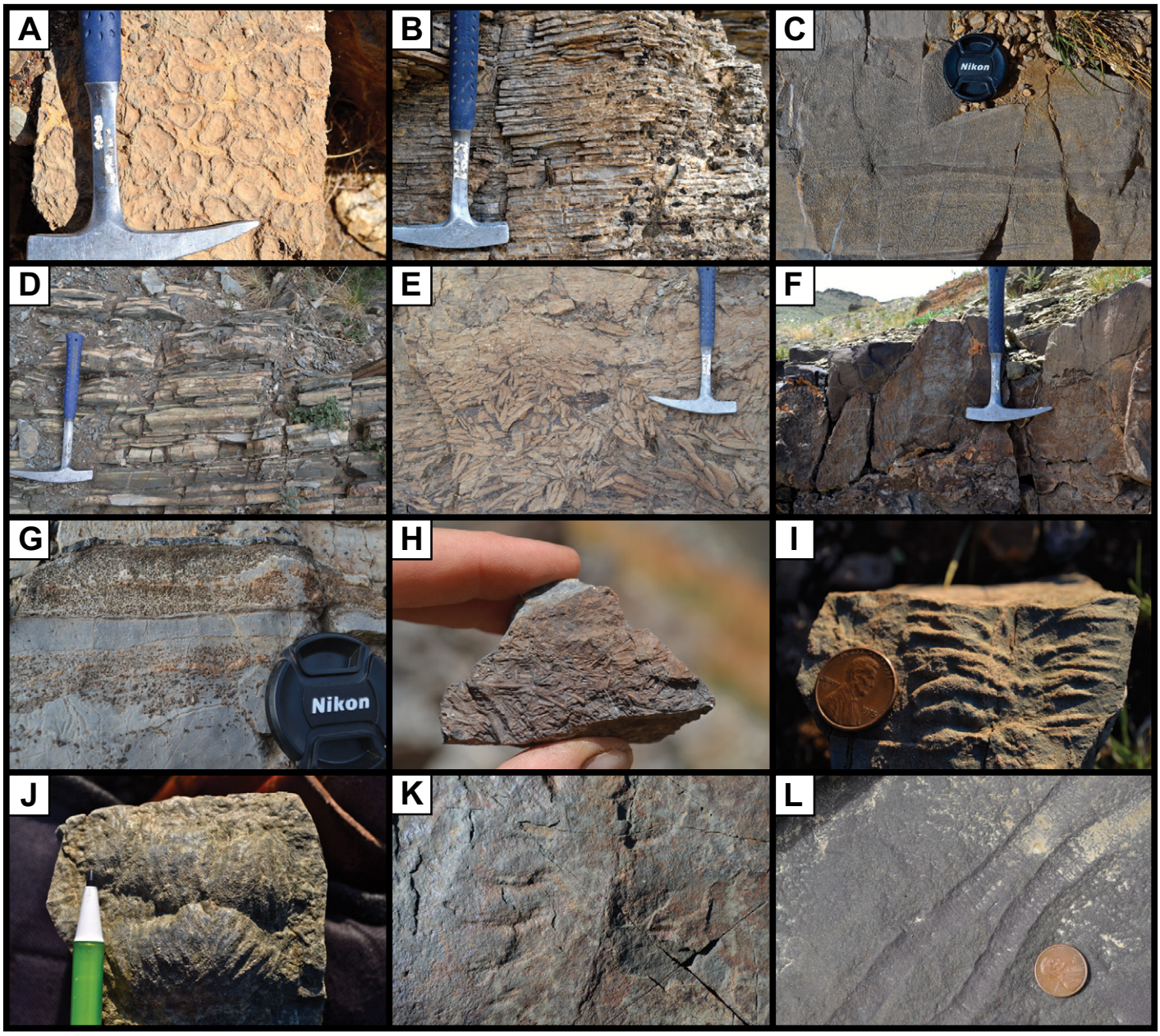

Figure 3. Photomontage of the Zuun-Arts and Bayangol Formations. (A) Stromatolite *Boxonia grumulosa* from the base of the Zuun-Arts Formation. (B) Thinly bedded, medium-gray limestone of lower to middle Zuun-Arts Formation. (C) Cross-bedded ooid grainstone of upper Zuun-Arts Formation. (D) Phosphatic shale with nodular limestone of lower Bayangol Formation. (E) Intraclast conglomerate in lower Bayangol Formation. (F) Thrombolites in upper part of Bayangol Formation in Bayan Gorge. (G) Phosphatized small shelly fossils, grains, and ooids in lag deposit in basal part of Bayangol Formation (137 m above basal contact) in Orolgo Gorge. (H) Anabaritids from basal Bayangol Formation in Orolgo Gorge. (I–K) Early arthropod trace fossils from the middle and upper Bayangol Formation (BG3–BG5) in Khunkher Gorge. (L) Bed-planar trace fossil from the upper Bayangol Formation (BG5) in S. Bayan Gorge.

graphic correlations. However, as discussed later herein, these lithostratigraphic correlations were compromised by large lateral facies changes. These lithostratigraphic correlations utilized the numbered units of Voronin et al. (1982) and were followed by the authors in the series of 1996 *Geological Magazine* publications. Although these numbered units are useful in identifying specific beds within a single gorge, they cannot be used to construct an accurate framework for basinwide correlations.

Salaagol Formation

The Salaagol Formation is a <400-m-thick white, gray, pink, and red microbial and archaeocyathan reef (Figs. 5A and 5B) that has only been described in detail from Salaa Gorge and Zuun-Arts Ridge (Voronin et al., 1982; Wood et al., 1993; Kruse et al., 1996). It has variably thick red silts and conglomerate interbeds. The formation also contains other bioclastic debris that includes chancellorid sclerites, sponge spicules, coralomorphs, and hyoliths (Kruse et al., 1996). The archaeocyathan assemblage at Salaa

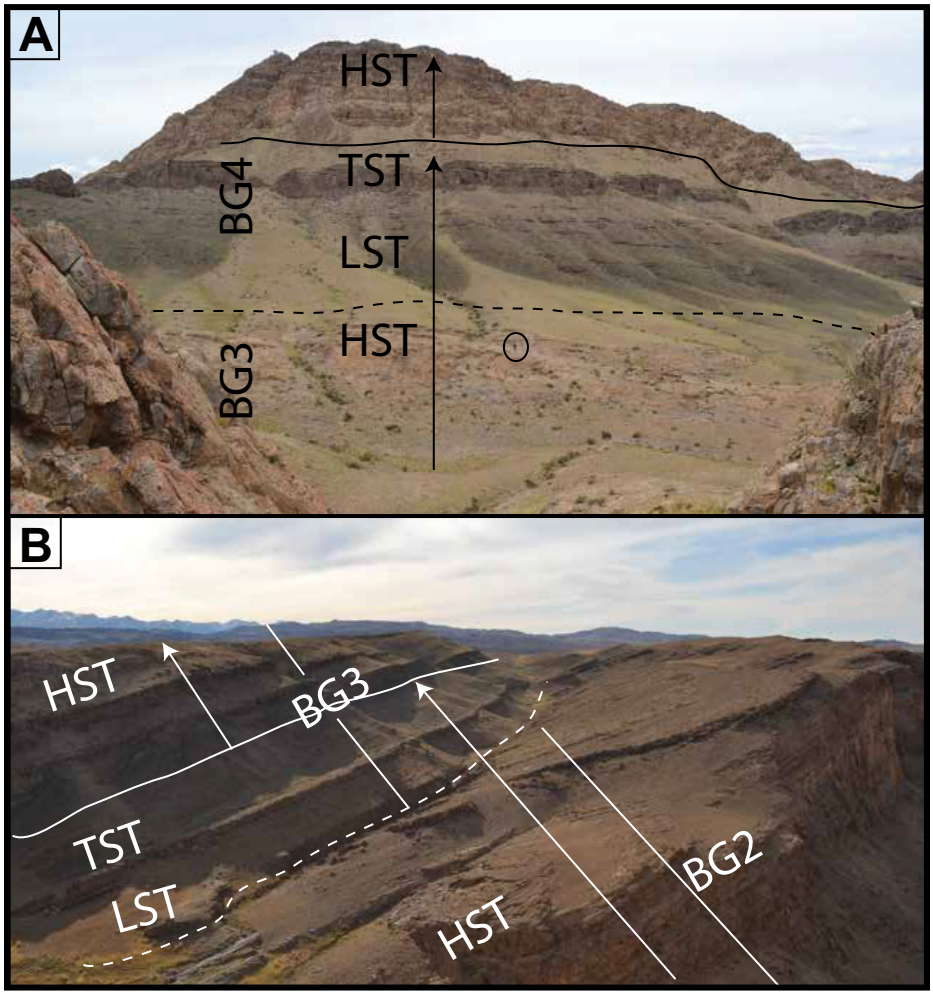

Figure 4. (A) Annotated photo looking to the NW in section E1211, NE of Khukh-Davaa Pass. The major sequence stratigraphic systems tracts of members BG3 and BG4 of the Bayangol Formation that are shown in Figure 7 are depicted here (the solid black line marks the maximum flooding surface, and the dashed line marks the boundary between BG3 and BG4). The dominant facies associations are also shown; however, it is not possible to mark all the facies associations at this scale. Human circled for scale. (B) Annotated photo looking to the west in the southern block of the Bayan Gorge. Major sequence stratigraphic systems tracts and facies associations of the lower two members of the Bayangol Formation are depicted here (the solid white line marks the maximum flooding surface, while the dashed line marks the top of BG2). Minor facies associations are not shown. HST—highstand systems tract; TST—transgressive systems tract; LST—lowstand systems tract.

Gorge is typified by *Archaeolynthus*, *Dokidocyathus*, *Nochoroicyathus*, and *Rotundocyathus*, and based on archaeocyathan biostratigraphy, Kruse et al. (1996) assigned it a Tommotian to Botomian age.

Khairkhan Formation

The Khairkhan Formation has only been described in Salaa Gorge as a >200 m siliciclastic succession that unconformably overlies older units (Voronin et al., 1982; Dorjnamjaa and Bat-Ireedui, 1991; Kruse et al., 1996). Our mapping and measured sections across the terrane demonstrate that the Khairkhan Formation is locally much thicker and consists of mixed siltstone, sandstone, and conglomerate, often containing large boulders of carbonate of the Salaagol Formation and chert and basalts clasts of unknown provenance. The Khairkhan Formation is the youngest Cambrian unit in the Zavkhan terrane, and has been interpreted as the mélange, flysch, and molasse of the foredeep (Macdonald et al., 2009). This interpretation is further supported by the structural position of the Khairkhan Formation at Orolgo Gorge (Figs. 1 and 6E), where it is overthrust by a klippe of ultramafic cumulates and serpentinite.

METHODS

Geological Mapping

Geological mapping was conducted over the course of three summers between 2011 and 2013. The detailed geologic mapping presented here provides the necessary context for the lithostratigraphy, chemostratigraphy, and biostratigraphy presented in this study. Higher-resolution stratigraphic studies of previously described and undescribed sections would not have been possible without new geological mapping. We returned to the five key areas that were described in the 1996 *Geological Magazine* publications, Bayan Gorge, Kvetee Tsakhir Nuruu, Orolgo Gorge, Salaa and Tsagaan Gorges, and Taishir to remap those areas in greater detail (Figs. 6A, 6B, 6C, and 6E). Additionally, we mapped many other parts of the Zavkhan terrane, targeting areas with good exposure and continuous sections of the Zuun-Arts, Bayangol, and Salaagol Formations (Figs. 6A, 6C, 6D, and 6E). Geological mapping enabled measurement of stratigraphic sections in the new, previously undescribed areas with the goal of putting together a more complete basinwide facies model and to construct a chemostratigraphic age model. Geologic mapping was conducted using LANDSAT satellite imagery, which offered the highest-resolution imagery available at the time.

For mapping purposes and sequence stratigraphic correlation, we informally divided the Bayangol Formation into five different members (BG2–BG6), of which the lower three members are capped by massive carbonate units that are clearly visible in satellite imagery (Fig. 4). When we initially divided units in the late Ediacaran to early Cambrian strata, we used BG1 interchangeably with Zuun-Arts because the Zuun-Arts Formation marks the onset of basin formation and is genetically related to the Bayangol Formation (Bold et al., 2013). Here, we use Zuun-Arts Formation in place of BG1. As the result of our detailed stratigraphic and mapping work, we have defined eight structural blocks (Taishir, Salaa, Tsakhir, Khavchig, Tsagaan, Orlogo, Khunkher, and South Khukh Davaa) that are characterized by distinct stratigraphy and are bounded by major faults (Fig. 1A).

Facies Associations and Sequence Stratigraphy

Nine facies associations were identified in this succession (Table 1), and for ease of discussion, they are grouped into five broad

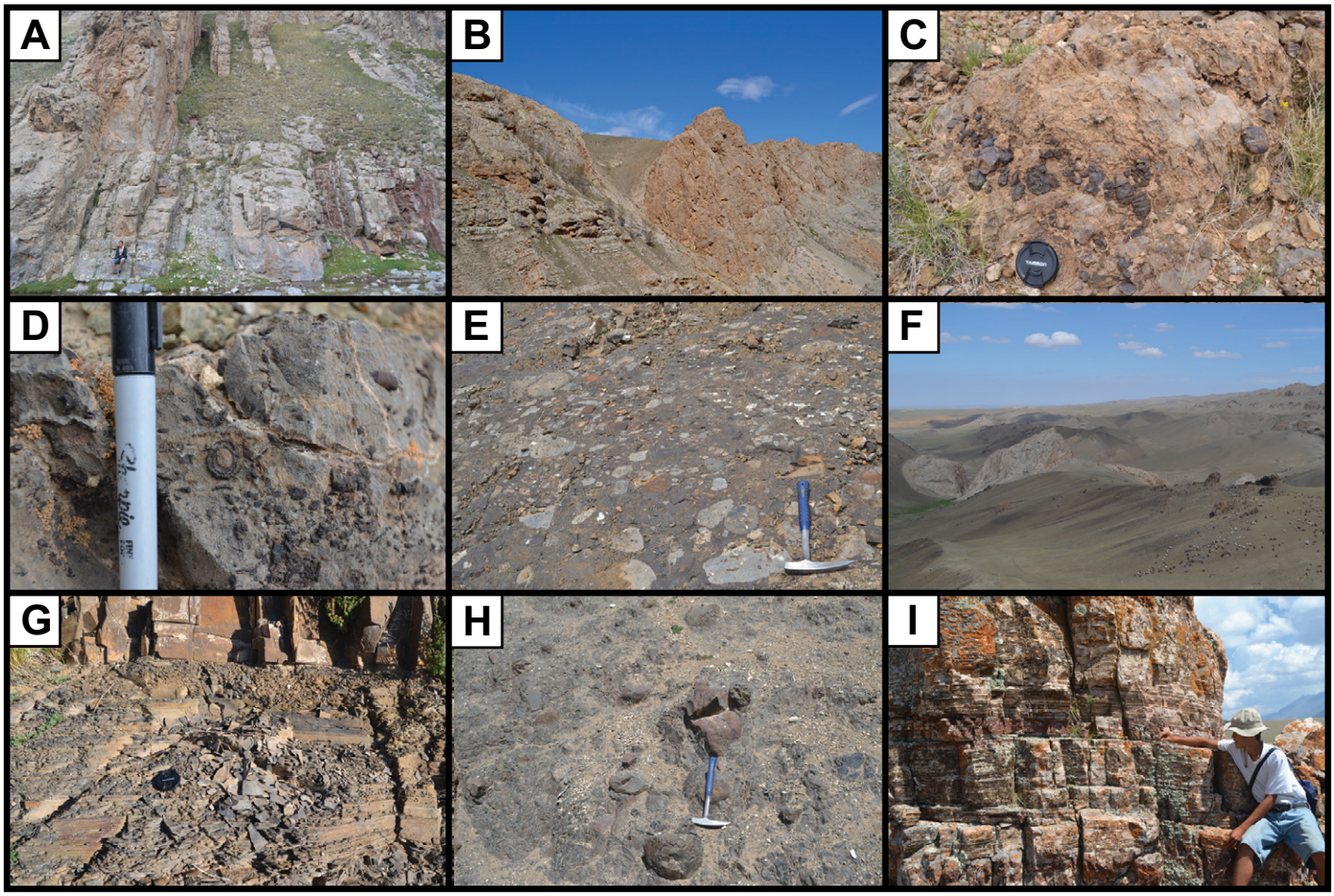

Figure 5. Photomontage of the Salaagol and Khairkhan Formations. (A) Interbedded microbial limestone and red silt near the base of the Salaagol Formation in Orolgo Gorge. (B) The upper Salaagol Formation (E1109) in Salaa Gorge with a goatherd for scale. (C) Rounded quartzite cobbles on top bedding surface of archaeocyath reef south of Khukh-Davaa Pass. Camera lens cap for scale. (D) Phosphatized grains, small shelly fossils, and archaeocyaths at top of Salaagol Formation south of Khukh-Davaa Pass. (E) Very poorly sorted, matrix-supported Khairkhan Formation conglomerate in Orolgo Gorge. Limestone clasts contain archaeocyaths. (F) Building-size olistolith of Salaagol Formation in Khairkhan Formation west of Orolgo Gorge. Goatherd for scale. (G) Black to brown silt of upper Khairkhan Formation south of Khukh-Davaa Pass. (H) Very poorly sorted, matrix-supported Khairkhan Formation conglomerate NW of Orolgo Gorge. (I) Partially silicified red- to buff-colored microbial dolostone of unknown age.

categories: (1) carbonate-dominated facies associations that were deposited on an outer-shelf to slope environment below storm wave base, (2) siliciclastic-dominated associations that were deposited on an outer-shelf to slope environment below storm wave base, (3) carbonate-dominated facies associations that were deposited in shelf to shoreface environments, (4) siliciclastic-dominated facies associations that were deposited in shelf to shoreface environments, and (5) flysch and mélange facies associations that were deposited during the terminal closure of early Cambrian orogenesis. These facies associations were used to identify the major stratigraphic sequences boundaries in the Zuun-Arts through Salaagol Formation succession.

The late Ediacaran to early Cambrian succession on the Zavkhan terrane contains multiple sequences that are appropriate for high-resolution sequence stratigraphy. In our analysis, we use the four commonly recognized system tracts: lowstand systems tract (LST), transgressive systems tract (TST), highstand systems tract (HST), and falling-stage systems tract (FSST), following Van Wagoner et al. (1990). We interpret carbonate deposition to represent TSTs and HSTs of relative sea level in the basin (Vail et al., 1977). For the carbonate-dominated slope facies in the lower to middle Zuun-Arts and lowermost Bayangol Formations, we utilize the TSTs and HSTs for correlation across the basin. The rest of the sequence contains abundant parasequences and bypass channels, so to pick out the major sequence boundaries, we use the LSTs, which are marked by an influx of medium to coarse sandstone and conglomerate across the basin (Vail et al., 1977; Mullins et al., 1987; Spence and Tucker, 1997).

$\delta^{13}C$ Chemostratigraphy

To test regional and global correlations, we sampled limestone spanning the Zuun-Arts Formation through the Salaagol Formation from across the Zavkhan terrane. Limestone rocks were sampled at 0.5–4 m resolution from 14 composite stratigraphic sections, many of which are composite sections (exact locations of measured sections are indicated in Fig. 6). Clean

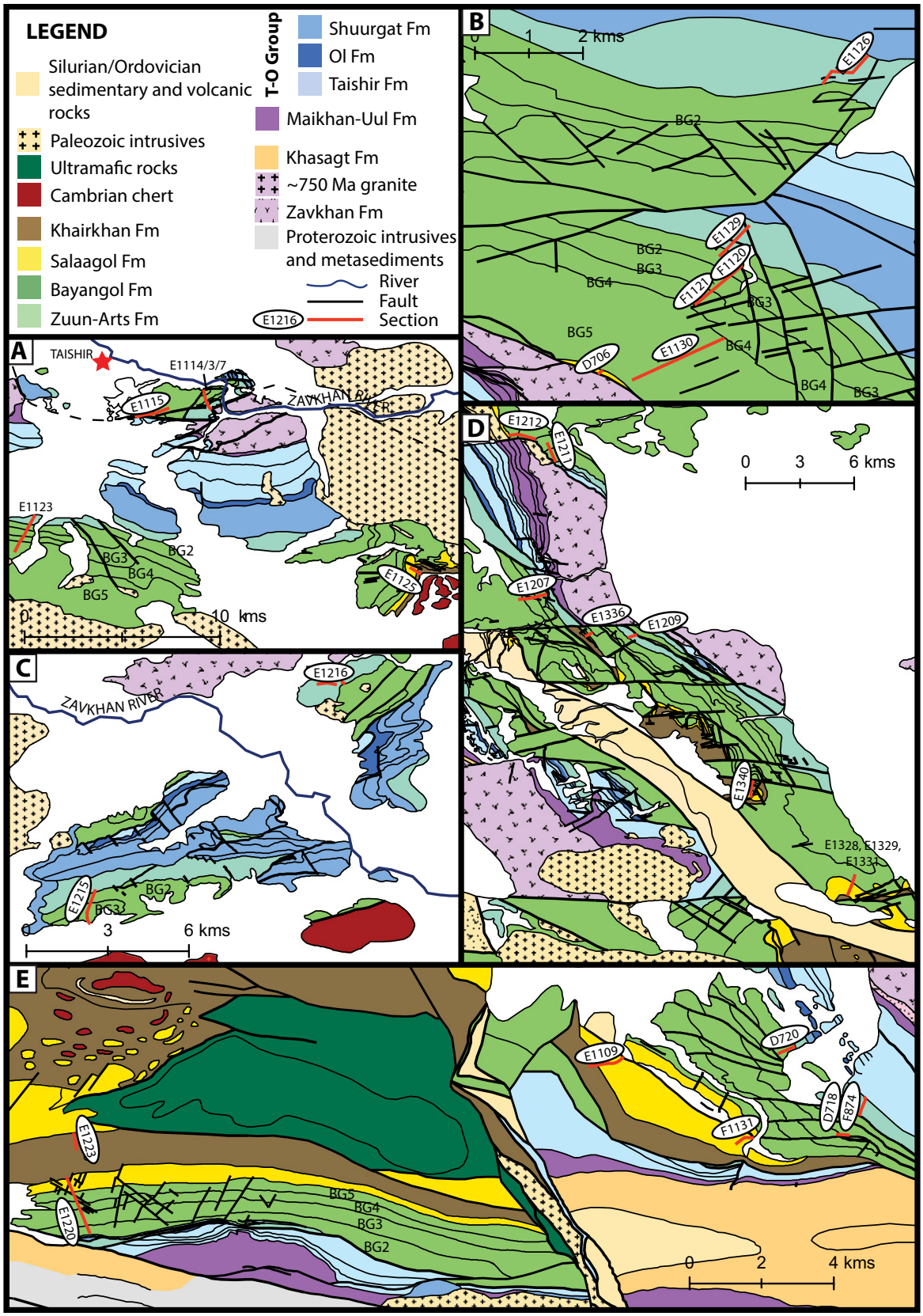

Figure 6. Detailed geological maps from across the Zavkhan terrane. Locations of maps are indicated in Figure 1. (A) Geological map of area SE of Taishir. (B) Geological maps of the southern and northern fault blocks in Bayan Gorge. (C) Geological maps of Kvetee Tsakhir Nuruu. (D) Geological map of Khukh-Davaa Pass (NW of town of Jargalant). (E) Geological maps of Orolgo, Salaa, and Tsagaan Gorges.

TABLE 1. FACIES ASSOCIATIONS FOR LATE EDIACARAN TO EARLY CAMBRIAN STRATA

Association	General character	Grain size	Bed thickness	Sedimentary structures	Origin and depositional environment
FA1: Thinly and well-bedded limestone	Clean, well-bedded medium- to dark-gray limestone; sometimes interbedded with very minor shale	Lime mudstone to wackestone	Very thin to thin; 1–5 cm thick	Rare slump folding; rare possible hold fast imprints and bed-planar trace fossils; rare stromatolites	Pelagic setting; deposited by turbidity currents on outer shelf to lower continental slope; deposited below storm wave base
FA2: Parted to ribbon-bedded limestone	Interbedded medium-gray limestone and mudstone	Lime mudstone to wackestone; partings are of shale to siltstone	Very thin to thin; 1–10 cm thick	Rare slump folding; rare possible Ediacaran fossils and bed-planar trace fossils; rare stromatolites	Pelagic to hemipelagic setting; deposited by turbidity currents on outer shelf to lower continental slope; deposited below storm wave base
FA3: Slope-derived carbonate breccia	Intraformational limestone tabular breccia; clasts derived from facies associations (FAs) 1 and 2; laterally discontinuous	Packstone; limestone clasts with lime matrix	0.1–5 m thick; laterally discontinuous	Clast to matrix supported	Deposited on a continental slope by debris flow
FA4: Phosphatic shale to siltstone	Phosphatic shale to siltstone with minor nodular limestone; minor amounts of phosphate	Microcrystalline shale with minor amounts of phosphate	1–20 m thick	Limestone nodulates; rare phosphatic hardgrounds with phosphatic grains, ooids, and small shelly fossils	Deposited in continental slope environments during marine transgressions
FA5: Turbiditic siltstone and sandstone	Interbedded siltstone and sandstone with isolated limestone beds	Siltstone to medium-grained sandstone	Thin to medium	Normally graded beds; load structures	Deposited on continental slope via dilute turbidity currents
FA6: Oolitic to oncolitic limestone	Limestone containing ooids and oncoids; thickly bedded	Packstone to grainstone	Thin to very thickly bedded	Trough cross-bedding	High-energy carbonate shoal
FA7: Platformal limestone	Massive microbialaminite, stromatolite, thrombolite, and archaeocyath reef. Light-gray limestone occasionally with minor sandstone to siltstone beds	Boundstone to bindstone	Thin to very thickly bedded	Bioturbation, stromatolites, thrombolites, archaeocyaths, nonphosphatized small shelly fossils rarely preserved; rare vugs	Deposited on carbonate shelf
FA8: Cross-bedded to swaley bedded sandstone	Bedded sandstone	Very fine to very coarse sand, dominantly fine to medium; locally contains dolomitic matrix	Thin to medium	High-angle trough cross-bedding; parallel laminations; ripple cross-lamination; bioturbation common	High-energy shoreface
FA9: Massive to graded conglomerate	Very poorly sorted, thickly bedded conglomerate	Poorly sorted sand matrix with pebble to boulder size clasts; olistoliths present locally	Medium to very thickly bedded	High-angle cross-bedding; unit bases erosional; laterally discontinuous; building-size olistoliths	Deposited by high-density turbidity currents in submarine channels; molasse and flysch deposits

limestone samples without siliciclastic components, secondary veining, or cleavage were targeted while sampling.

Carbon ($\delta^{13}C$) and oxygen ($\delta^{18}O$) isotopic measurements were obtained on 2763 samples. Samples were microdrilled along individual laminations, where visible, to obtain 5–20 mg of powder. Veins, fractures, and siliciclastic-rich areas were avoided. Carbonate $\delta^{13}C$ and $\delta^{18}O$ data were acquired simultaneously on a VG Optima dual-inlet mass spectrometer at the Harvard University Laboratory for Geochemical Oceanography. Carbonate samples were reacted with orthophosphoric acid using a VG Isocarb preparation device, which includes a common acid bath with a magnetic stirrer. Approximately 1 mg of microdrilled samples was reacted in the bath at 90 °C. Evolved CO_2 was collected cryogenically and analyzed using an in-house reference gas. Potential memory effect resulting from the common acid-bath system was minimized by increasing the reaction time for dolomite samples. Memory effect is estimated at <0.1‰ based on variability of standards run after dolomite samples. Standard deviation (1σ) from standards was better than ±0.1‰ for both $\delta^{13}C$ and $\delta^{18}O$. Carbonate $\delta^{13}C$ and $\delta^{18}O$ isotopic results are reported in per mil (‰) notation relative to VPDB (Vienna Peedee belemnite) by using an in-house Carrara Marble standard that was calibrated against several NBS carbonate standards and cross-calibrated with other laboratories.

Constructing an Age Model

Because global stages 2–4 of the early Cambrian have not been defined yet, and previous global correlations of early Cambrian data use stratigraphic terminology from Siberia and Kazakhstan, for the sake of consistency, we also use the stage system for the Lower Cambrian on the Siberian Platform in this study. The Lower Cambrian on the Siberian Platform is divided into the Nemakit-Daldynian, Tommotian, Atdabanian, Botomian, and Toyonian (Repina and Rozanov, 1992; Rozanov et al., 2008). Generally, the Nemakit-Daldynian and Tommotian are thought to be correlative with the Terreneuvian Series. The Atdabanian and Botomian are thought to be correlative with the undefined Series 2 of the early Cambrian.

Similar to the way in which previous workers created composite $\delta^{13}C$ curves and correlated sections globally, a combination of positive and negative excursions was used as tie points in this study. These $\delta^{13}C$ excursions were first labeled in Siberia (e.g., Kouchinsky et al., 2007) and have been used in several global compilations since. With these data, 1n, the most negative

$\delta^{13}C$ value at the Ediacaran-Cambrian boundary, and five positive $\delta^{13}C$ excursions (2p–6p) were identified in each section. A composite $\delta^{13}C$ chemostratigraphic curve was constructed by stretching the $\delta^{13}C$ values between each of these tie points, assuming constant sedimentation rates in each section. Calibration points for positive excursions are the same as those used in Maloof et al. (2010a).

Paleontology

Body and trace fossils were sampled and photographed while measuring stratigraphic sections. This study places previously described small shelly fossil horizons into the necessary stratigraphic context and a refined age model. Revised mapping and correlation among sections have resulted in different interpretations of the stratigraphic position of the small shelly fossil horizons.

Small shelly fossil taxon names from previous small shelly fossil horizons were taken from the compilation done by Brasier et al. (1996b) and Khomentovsky and Gibsher (1996) and the publication by Esakova and Zhegallo (1996). For generic and higher group assignments for individual taxa, we followed the supplementary material of Maloof et al. (2010a, and references therein).

RESULTS

Reconstructions of the Zavkhan Terrane

Based on geological mapping, we identified major faults in the Zavkhan terrane (Fig. 1A) and grouped measured sections that are on the same fault block together. The southern thrust sheets preserve more distal sections, and the northern ones are more proximal. The measured sections presented here are ordered according to depositional paleodepth (Fig. 7). Next, we organize the results from more proximal to more distal.

Facies Associations

The facies associations (FAs) described next, grouped according to paleo–water depth, and the descriptions and environmental interpretations are summarized in Table 1.

Slope- to Outer Shelf–Deposited Carbonate Facies Associations

Three carbonate-dominated FAs show evidence of deposition in deeper-water slope to outer-shelf settings. These facies are characteristic of the lower to middle Zuun-Arts Formation.

Facies association 1. FA 1 is characterized by thinly bedded, normally graded packstone, wackestone, or lime mudstone with very minor amounts of siliciclastic material. Typi-

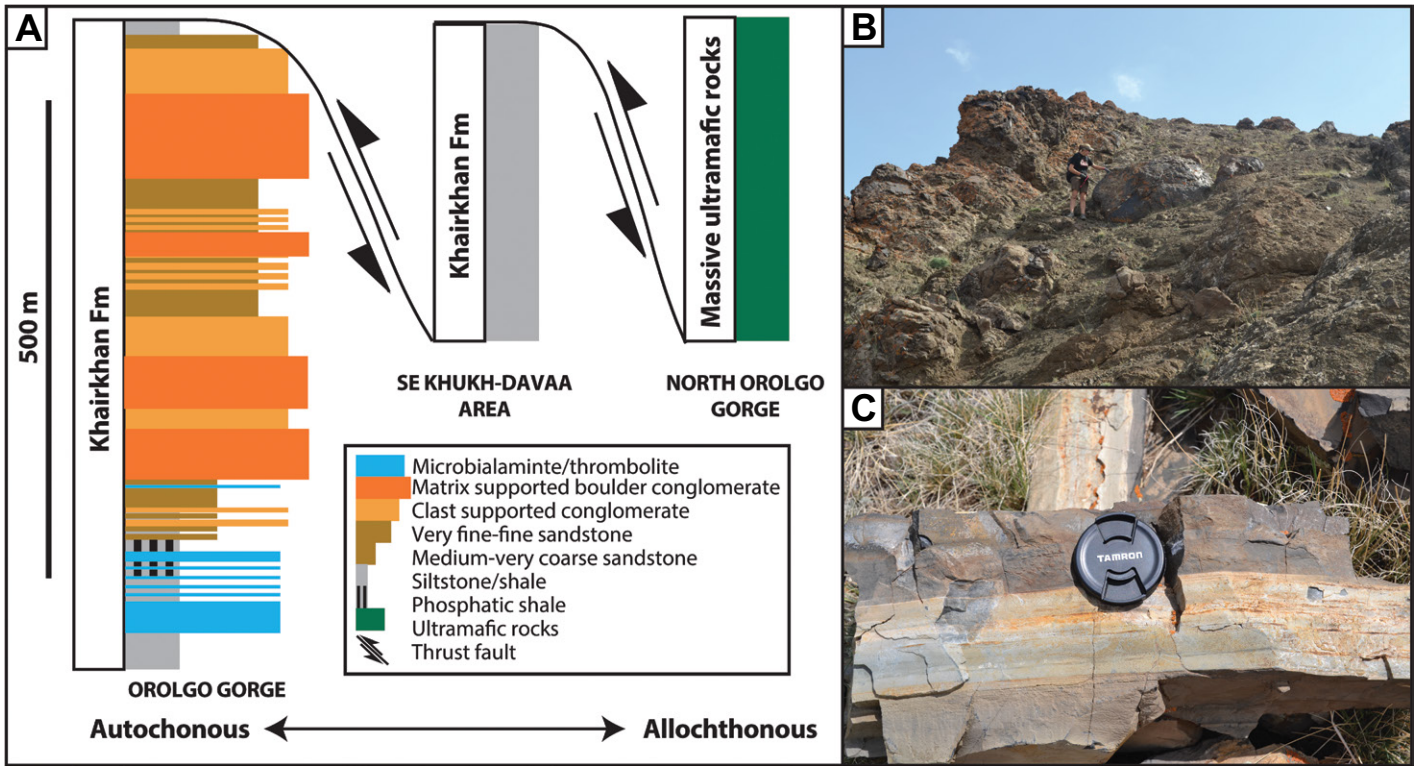

Figure 7. Integrated lithostratigraphy, sequence stratigraphy, and $\delta^{13}C$ chemostratigraphy of the Zuun-Arts and Bayangol Formations. Measured sections are numbered according to proximity to the paleoshoreline, with more distal sections on the right and more proximal sections on the left. Locations of the individual measured sections are shown on the map in the lower-left side of the figure. Small shelly fossils (SSFs) horizons from this study are marked with red stars, and those from previous studies are marked with green stars. Purple circles mark ichnofossil horizons. Previous paleontological data from Orolgo (Orolchayn) Gorge is revised from Endonzhamts and Lkhasuren (1988). Paleontological data from Salaa and Tsagaan Gorges are from Voronin et al. (1982), Esakova and Zhegallo (1996), and Khomentovsky and Gibsher (1996). The paleontological data from Bayan Gorge are from Khomentovsky and Gibsher (1996). Each of the previous small shelly fossil horizons is labeled according to the labeling schemes of the different collections. Shaded colored boxes show correlation between sections. VPDB—Vienna Peedee belemnite; HST—highstand systems tract; TST—transgressive systems tract; LST—lowstand systems tract.

cally, these beds are dark to light gray in color. The limestone beds have sharp bases and tops and are normally graded. Occasionally, soft sedimentary slumping is present. FA 1 is the dominant facies in the lower to middle part of the Zuun-Arts Formation and is interpreted to represent outer-shelf to upper-slope deposition below storm wave base.

Facies association 2. FA 2 is a ribbon-bedded limestone, similar to FA 1 in that is a thinly bedded, carbonate-dominated facies. Typically, these beds are medium to light gray in color. FA 2 differs from FA 1 in that it contains shale or siltstone partings. This facies association is common in the middle part of Zuun-Arts Formation as well as portions of the Bayangol Formation, and we interpret it to represent outer-shelf to lower-slope deposition below storm wave base.

Facies association 3. FA 3 is a slope-derived carbonate breccia that consists of clast- to matrix-supported intraformational limestone conglomerate. Clasts are tabular with composition similar to the underlying and overlying units and indicative of derivation from surrounding slope deposits. This type of sedimentary breccia is present in some sections of the lower Zuun-Arts Formation and lower Bayangol Formation. Some of the sedimentary breccias in the Zuun-Arts Formation are found in association with slump folding, suggesting that these breccias were deposited during slope failure. Other breccias could represent storm-dominated facies.

Slope-Deposited Siliciclastic Facies Associations

Facies association 4. FA 4 is present at the base of the Zuun-Arts and Bayangol Formations and is characterized by laminated phosphatic shale to siltstone. Locally, this FA is present at the contact between the Salaagol and Khairkhan Formations. Tan carbonate nodules in the shale and siltstone are locally present. Volumetrically, FA 4 is not a major component of the succession; however, it is a distinct and important stratigraphic marker.

Facies association 5. FA 5 is characterized by thinly bedded, finely laminated siltstone, turbiditic sandstones, and pebble conglomerates. Fining-upward sequences are common. Bouma units A–C (and D–E in some sections) are commonly preserved. FA 5 is present in the middle to upper part of the Khairkhan Formation.

Shelf to Shoreface Carbonate Facies Associations

Facies association 6. FA 6 is cross-bedded to swaley-bedded oolitic to oncolitic limestone. Occasionally, the oolitic limestone contains quartz grains. This facies is found in the uppermost Zuun-Arts Formation, throughout the Bayangol Formation, and in parts of the Salaagol Formation.

Facies association 7. FA 7 is anything ranging from microbialaminites, stromatolites, and thrombolites to an archaeocyath reef. Different microbial and thrombolitic textures are common throughout the Bayangol Formation and parts of the Salaagol Formation. The Salaagol Formation also contains beautifully preserved archaeocyath and hyolith reefs that range in size from laterally discontinuous patch reefs to hundreds of meters thick and for more than a kilometer along strike.

Shelf to Shoreface Siliciclastic Facies Associations

Facies association 8. FA 8 is a cross-bedded to swaley-bedded sandstone. It is characterized by finely to thickly bedded, very fine- to very coarse-grained quartzarenite to calcarenite. Sedimentary structures include high-angle cross-stratification, parallel bedding, current ripples, and normally graded beds. Bioturbation is common is this FA. FA 8 is found throughout the Bayangol Formation.

Facies association 9. FA 9 is an immature, poorly sorted pebble to boulder conglomerate. Conglomerates are found in the Bayangol through Khairkhan Formation but differ in texture, composition, and thickness. The Bayangol Formation contains centimeter-thick lenticular pebble conglomerates. Often, these conglomerates are red-colored and feldspathic, and they can contain phosphatized grains and small shelly fossils. In the Salaagol Formation, there is a wide range of conglomerates that include centimeter-thick pebble conglomerates with angular clasts to cobble conglomerates that are tens of meters thick with rounded clasts of underlying strata. These conglomerates occur between archaeocyath reefs. Additionally, this facies is found in the shallow-water facies of the Khairkhan Formation, and it is interpreted as the molasse of the foreland.

Key Locations: Geologic Mapping, Sedimentology, and Stratigraphy

Next, we present the results of geological mapping (Figs. 1 and 6), sedimentology, and stratigraphy that have enabled the refinement of the small shelly fossil biostratigraphy in the Zavkhan Basin. These results are synthesized for each locality. In some cases, the geological mapping has greatly changed the interpretation of the stratigraphy, including the small shelly fossil biostratigraphy and the chemostratigraphy. The deformation in the Zavkhan terrane is almost entirely brittle deformation and, generally, is dominated by a conjugate set of right-lateral strike-slip faults and oblique en echelon thrust faults.

Taishir (E1114, E1113, E1115, E1117, E1325)

Most previous studies at this locality focused on the underlying Tsagaan-Olom Group (Goldring and Jensen, 1996; Khomentovsky and Gibsher, 1996; Macdonald et al., 2009; Macdonald, 2011) and the fossils, bioherms, and patch reefs of the Bayangol Formation (Dorjnamjaa and Bat-Ireedui, 1991; Goldring and Jensen, 1996; Kruse et al., 1996). Detailed mapping of the Zuun-Arts and Bayangol Formations just to the southeast of the town of Taishir allowed us to measure a composite section of the two formations at this locality and to place previously poorly contextualized fossil horizons into a coherent stratigraphic framework. Additional geologic mapping to the SSW and SW of the town of Taishir led to the discovery of more previously unreported, well-exposed sections. Sections of the Zuun-Arts and Bayangol Formations are well-exposed to the SSW in a low creek bed (Fig. 6A). Additionally, just south of the large Permian intrusion, sections of the Upper Bayangol through Khairkhan Formations are well exposed. All of these sections described here are on the same fault block as the Bayan Gorge sections.

One of the measured sections of the Zuun-Arts Formation, E1114, was measured near the town of Taishir. Section E1114 was measured just south of the Zavkhan River and east of the town of Taishir. The total measured thickness of E1114 is 176 m. Only the top surface of the stromatolite *Boxonia grumulosa* is exposed in a gully. Brown and black, cherty, phosphatic shale overlies the buff- to pink-colored *Boxonia grumulosa*. Similar to the Bayan Gorge sections, the basal portion of this section is dominated by very thinly bedded limestone with nodular and bedded chert and abundant interclast breccia beds that pinch out laterally. The top 24 m portion of the Zuun-Arts Formation is light-gray cross-bedded ooid grainstone.

For the Bayangol Formation, Kruse et al. (1996) presented a 30 m section, which they referred to as "Tayshir I" (not to be confused with the Tayshir I and II sections of the Maikhan Uul and Taishir Formations in Khomentovsky and Gibsher [1996]), which we mapped as members BG2 and BG3. They also described two 7 m sections that they called "Discovery site" and "Ovoo site," and which we interpret as being a portion of BG4 in our section E1115. However, without much context, it is difficult to know exactly where these previously measured

sections are. The fossil horizons from Taishir are not included in previous small shelly fossil biostratigraphic compilations (i.e., Khomentovsky and Gibsher, 1996; Maloof et al., 2010a). Here, we present a composite measured section of the Bayangol Formation (E1113, E1115, and E1117) that enables us to put new and previous fossil finds into the correct stratigraphic context.

Members BG2 through lower BG4 sit conformably above the Zuun-Arts Formation in a well-exposed section to the south and west of a bend in the Zavkhan River. The rest of the Bayangol section (very upper BG3 through BG5) is exposed in a broad syncline to the west of a left-lateral strike-slip fault. There is a poorly sorted red conglomerate overlain by elongate stromatolites at the BG3-BG4 contact that were used to tie the sections together. Member BG5 is very shallowly dipping near the top of the section, and the upper contact of the formation is not exposed.

Members BG4 and BG5 of this section (E1115) have some exceptional features, including abundant and diverse trace fossils and small shelly fossil assemblages. The elongation of the stromatolites at the base of BG4 is oriented at 210°, an indicator that the paleoshoreline was oriented perpendicular to the direction of elongation along a NW-SE transect in modern coordinates (Hoffman, 1967). The upper part of BG5 is notable because of its >100 m of siltstone to sandstone beds that contain few sedimentary features. Some of the beds are slightly graded, but many are structureless medium to coarse sandstone units that lack bedding surfaces.

Just SE of Taishir, there is an excellent section of the Salaagol Formation called E1325. The basal contact of the Salaagol Formation is not exposed at this section, but laterally, it rests conformably on a white to pink quartz pebble conglomerate. The Salaagol Formation is 177 m thick at this locality. The basal ~38 m section of the formation consists of microbialaminite and massive recrystallized limestone. The recrystallization is patchy and is most likely the result of the contact metamorphism from nearby intrusion. At 38 m above the base of the formation, well-preserved archaeocyaths appear, and at 84 m, they are the dominant reef former.

The Khairkhan Formation rests conformably on top of the Salaagol Formation at this locality. Just to the south of E1325, this formation is better exposed as a poorly sorted, very coarse sandstone to pebble conglomerate. The top contact of the Khairkhan Formation is not exposed anywhere in this area. There is ~10–20 m of nonexposure between the top contact of the Khairkhan Formation and a red to black chert of unknown age.

Kvetee Tsakhir Nuruu (E1216, E1215, E1217, E1219)

This ridge is located ~30 km southeast of the town of Taishir on the south side of the river (Fig. 6C). The Zuun-Arts Formation and the basal Bayangol Formation are exposed on the southwestern side of the ridge. Additional mapping northeast of the river resulted in the discovery of a well-exposed section of the Zuun-Arts Formation (E1216) and a well-exposed but faulted and folded section of the lower Bayangol Formation (E1215, E1217, E1219).

Phosphatic shale and subcrop of thinly bedded limestone mark the base of the Zuun-Arts Formation at this locality. *Boxonia grumulosa* is present in other sections at Kvetee Tsakhir Nuruu but is not exposed at the exact place in which this section was measured. The basal 50 m portion of this measured section is thinly bedded limestone with black, phosphatic shale and minor intraclastic breccia. The black shale here was thicker and more abundant than in any other section. The middle part of the section is dominated by thinly bedded limestone with more intraclastic breccia and slump folding with vergence to the southeast (n = 41). The top of the section contains more thinly bedded limestone and debris flows but also abundant sandstone and siltstone interbeds. This is the only section in which sandstone, siltstone, and shale were observed at the top of the section instead of cross-bedded ooid grainstone.

The measured section of the Bayangol Formation (E1215) is the same section as the previously described section at Kvetee Tsakhir Nuruu, south of the Zavkhan River (Zhegallo and Zhuravlev, 1991; Dorjnamjaa et al., 1993; Brasier et al., 1996b). At this locality, the Bayangol Formation is relatively thin, and only the basal part is exposed. The base of the section is marked by thinly bedded limestone that grades up into massively weathering, partially recrystallized limestone that looks similar to the upper part of the Zuun-Arts Formation. This limestone is capped by shale, an obvious lenticular pebble conglomerate that contains phosphatized ooids and small shelly fossils, and bioturbated limestone.

More strata of the Bayangol Formation are exposed north of the Zavkhan River, where the basal contact with the Zuun-Arts Formation is clearly exposed. However, there, much of the Bayangol Formation strata are faulted, folded, relatively flat-lying, and massively weathering, preventing us from measuring a complete section of the formation. Sections E1217 and E1219 (not plotted in Fig. 7) comprise a composite section of BG2 and BG3 strata. E1217 sits conformably on E1216, the measured section of the Zuun-Arts Formation described already, and E1219 is a measured section of member BG3, exposed in the limb of a syncline.

SE of Bayan Gorge (E1123)

South of the town of Taishir and SE of Bayan Gorge, there is a previously undescribed, well-exposed section of the Bayangol Formation (E1123). Because this section is on the same fault block as the southern Bayan Gorge section, it is similar in facies and has similar thickness to the composite section there.

The basal portion of the Zuun-Arts Formation is not well exposed at this locality, so only the upper 106 m portion was measured. The beds in this section are shallowly dipping, and the exposure of this section is not as good as the exposures in Bayan Gorge or Taishir. Nonetheless, the section offers another opportunity to measure and sample the middle to upper part of the Zuun-Arts Formation. The measured thickness of BG2–BG4 here is 357 m, and sedimentologically, it is very similar to the measured section in Bayan Gorge. The upper part of the formation (BG5) was not measured in detail at this locality, because, due to a major fault, there is no top contact with the Salaagol Formation.

Bayan Gorge (E1126, E1129, F1120, F1121, E1130, D706)

The Bayan Gorge is on the south side of the Zavkhan River, ~15 km west of Taishir (Fig. 6B). It hosts a northern and southern fault block of very well-exposed sections of the Zuun-Arts and Bayangol Formations. Despite abundant, but minor, conjugate fault sets in the gorge, the mapping is tractable. We present revised maps of Bayan Gorge and used this new mapping to construct a composite section of the Zuun-Arts (E1129 from the southern block) through Bayangol Formations (F1120, F1121, E1130, and D706 from the northern block). Previous workers suggested that in the southern fault block, there was repetition of the lower Bayangol Formation (their units 17 and 18, our BG2) due to thrust faults (Gibsher et al., 1991; Khomentovsky and Gibsher, 1996); however, we observed only small offsets due to the conjugate sets of faults. Importantly, this revised mapping changed the stratigraphy and placement of small shelly fossil horizons into the composite small shelly fossil range chart. Instead of repeating strata (units 17 and 18, our BG2), on the west side of the gorge, we observed continuous stratigraphy that is much thicker than previously reported.

Two sections of the Zuun-Arts Formation, one on the southern fault block (E1129) and the other on the northern fault block (E1126), were measured in Bayan Gorge; however, the data in Figure 7 are from E1129. The two sections are

both very well exposed with similar thickness and stratigraphy.

Beginning at the top contact of the stromatolite *Boxonia grumulosa*, the measured section on the southern block (E1129) is 221 m thick. The base of the section is marked by green phosphatic shale with bedded chert and nodular limestone that is overlain by thinly bedded limestone with bedded and nodular chert. The lower part of the Zuun-Arts Formation is predominantly thinly bedded (1–2 cm), dark-gray limestone (Fig. 3B) with 0.5–1.5 m beds of limestone interclastic breccia. In the middle to upper part of the Zuun-Arts Formation, there are several 5–15 m parasequences. The bases of the parasequence are marked by planar, thinly bedded limestone interbedded with pink calcisiltite. Up section, the beds become thicker, and the tops of some of the parasequences are capped by cross-bedded ooid grainstone.

Beginning at the top contact of the stromatolite *Boxonia grumulosa*, the measured section in the north block (E1126) is 203 m thick. This section is very similar sedimentologically to the section E1129. Well-preserved simple bed-planar trace fossils were found at 169 m. The upper contact with the Bayangol Formation is a sharp transgression between massive ooid grainstone of the Zuun-Arts Formation and green phosphatic shale interbedded with limestone of the basal Bayangol Formation.

The section of the Bayangol Formation on the southern block of Bayan Gorge is the most-studied section and the type locality of the Bayangol Formation. Two sets of unit numbering, painted onto the cliff faces, have been used by Zhegallo and Zhuravlev (1991) and Gibsher et al. (1991), which were subsequently used by Khomentovsky and Gibsher (1996). However, due to the mismapping of the gorge, we do not use either of the numbering schemes. The three thick carbonates that cap members BG2–BG4 are clearly visible in satellite imagery and are present in many other localities. This is an important distinction because previous writers have interpreted what we refer to as BG3 (units 18 and 19 in Gibsher et al., 1991) as being a thrust repetition of BG2. As a result, our measured section is thicker and contains additional strata that are missing in the middle of previous measured sections.

Khukh-Davaa

"Khukh-Davaa" is the name of the pass along a left-lateral, E-W–oriented, strike-slip fault in the northwestern Khevtee Tsakhir Range (Fig. 6D). New mapping in this area resulted in the discovery of many new sections of the late Ediacaran through early Cambrian stratigraphy both north and south of the Khukh-Davaa Pass. Geologic mapping was focused on the eastern side of the NW-SE Late Ordovician to Silurian graben. There is a major fault separating the NE section from the SE one, so the results from these two sections are discussed separately next. The SE section is interpreted to have been deposited on the same fault block as the section from Salaa and Tsagaan Gorges (Figs. 1A and 1D), whereas the NE Khukh-Davaa section is interpreted to be on the same fault block as the section from Khunkher Gorge. Based on mapping of these two fault blocks, we interpret the thrust sheet with the sections from SE Khukh-Davaa and Salaa and Tsagaan Gorges to be the more proximal of the two.

SE Khukh-Davaa (E1209, E1207, E1336, E1328, E1329, E1331, E1339, E1340)

The section of the Zuun-Arts Formation at this locality (E1209) is exceptional in several regards, including unusual sedimentary features and expanded portions of different parts of the formation. The total thickness of this measured section is 263 m. The base of the section is marked by a silicified karst surface followed by thinly bedded, graded dolosiltite and a 10 m horizon of *Boxonia grumulosa.* Capping the stromatolites are phosphatic shales interbedded with mechanically bedded light-gray dolostone. Overlying the basal interbedded phosphatic shale and dolostone, there is dark-gray to black, sulfidic limestone and dolostone with rare domal stromatolites. The top 134 m portion is dominated by cross-bedded limestone ooid and mudchip grainstone. Paleoflow of the cross-beds is to the southeast. The cross-bedded ooid grainstone shoal at the top of this section is much thicker here than it is in any other section measured.

The section of the Bayangol Formation is a composite section in which BG2–BG4 of the Bayangol Formation (E1207) were measured just north of Khukh-Davaa Pass, and the upper part (BG5) of the formation (E1336) was measured just south of the pass in a broad anticline. The two sections are separated by a left-lateral strike-slip fault; however, the offset of the fault is not major.

The base of E1207 is marked by an unusually thick section of red and green shale sharply overlying cross-bedded ooid grainstone of the upper Zuun-Arts Formation. There are many small, insidious faults and few distinct marker beds in the lowermost part of the Bayangol Formation in this section, and it is possible that the thickness in Figure 7 is exaggerated due to structural repetition of the shale beds. The top of BG2 is marked by a few small shelly fossil horizons interbedded with black shale and a phosphatic hardground. Similar to other sections, member BG3 at this locality is carbonate dominated in the middle part of the member, as well as the upper part. It has thick, bioturbated limestone beds, oncolites, and oolites that are interbedded with siltstone and fine to coarse sandstones in the lower to middle part of the member.

The base of section E1336 is marked by the resistant thick limestone unit that is just south of the left-lateral fault marking Khukh-Davaa Pass. This section is composed of predominantly green-colored, fine- to medium-grained sandstone. Here, 1–3 m microbial patch reefs and small centimeter-scale microbial balls with diffuse edges are present throughout the section. Additionally, coarse white quartzarenites become increasingly more dominant and coarser up section. In the 20 m below the first archaeocyath reef, the sandstone is white, medium to very coarse, and quartz dominated. We call this upper 20 m of the Bayangol Formation "member BG6"; however, the contact between BG5 and BG6 is gradational.

The Salaagol and Khairkhan Formations are well exposed in several localities south of the Khukh-Davaa Pass (Fig. 6D). Both formations are highly variable along strike, and two sections that capture that variability are presented here (Fig. 8). The Salaagol Formation ranges in thickness from 0 to 175 m. In many sections in this area, the limestone of the Salaagol Formation interfingers with siltstone, sandstone, and conglomerate that are lithologically similar to the overlying Khairkhan Formation. We define the top of the Salaagol Formation as the uppermost limestone unit. In some sections, the Salaagol Formation is composed of meter-scale patch reefs that pinch out laterally. In other sections, it is composed of ~10-m-scale archaeocyath reefs with ~50 m cobble conglomerates between (Fig. 5C). In still other sections, the Salaagol Formation is entirely absent, with a cobble conglomerate resting unconformably on very coarse quartz-rich sands of the upper Bayangol Formation.

In the thickest measured section of the Salaagol Formation (E1328 and E1329), the base of the Salaagol Formation is composed of thinly bedded, medium-gray limestone grainstone with ooids. At ~50 m, there is a gradational contact with ooid grainstone and thrombolites with occasional quartz pebble conglomerates. Further up section, thrombolitic and hyolith reefs dominate, with occasional sandstones and conglomerates. Dispersed archaeocyaths first appear at 111 m on the edges of stromatolites and become the dominant reef builders at 124 m. The upper 8 m portion of the section is thinly bedded limestone with glauconitic sandstone and phosphatic hardgrounds. Phosphatized and partially phosphatized hyoliths, chancelorids,

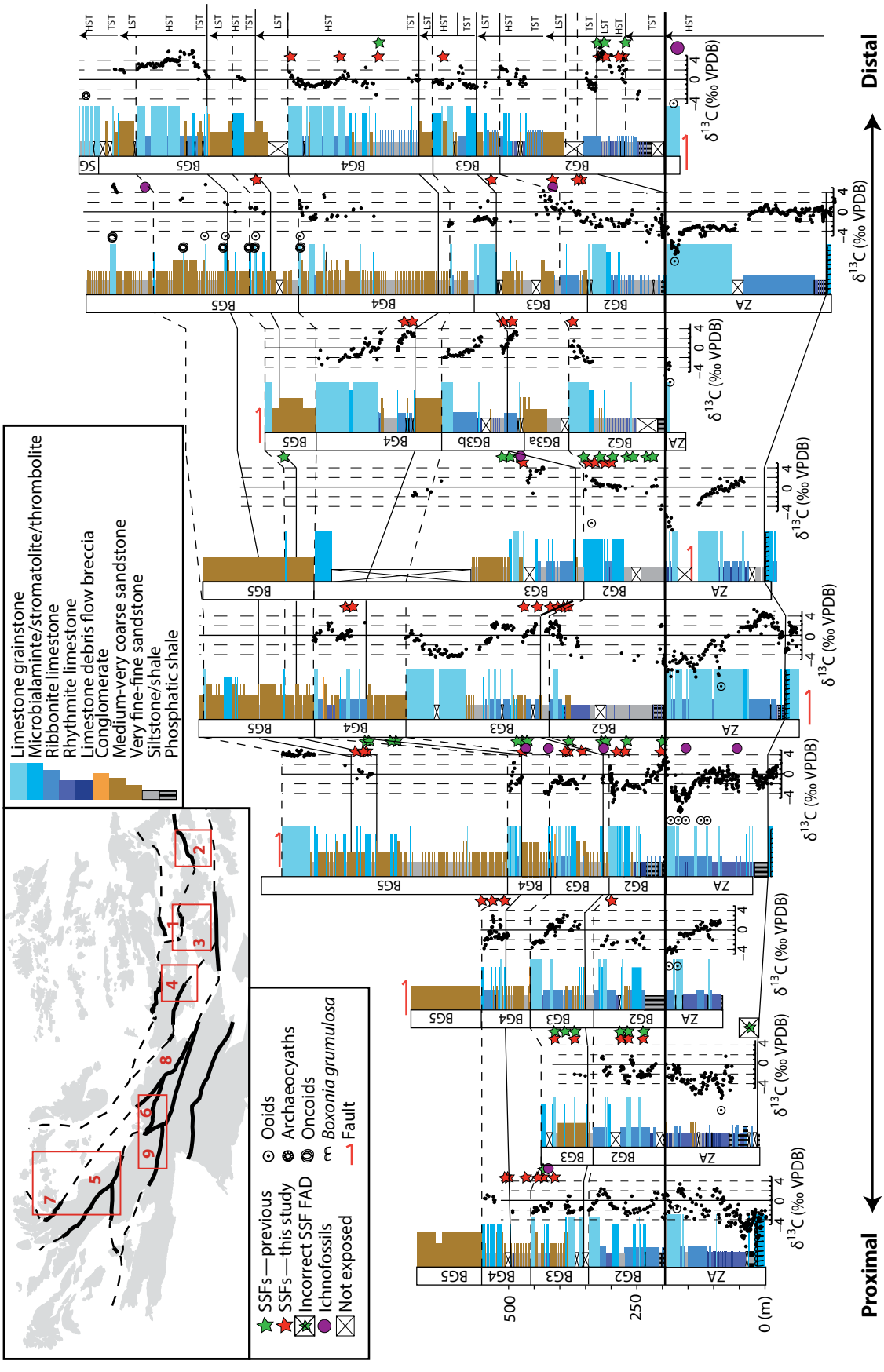

Figure 8. Integrated lithostratigraphy, sequence stratigraphy, and $\delta^{13}C$ chemostratigraphy of the uppermost Bayangol, Salaagol, and Khairkhan Formations. The five measured sections are numbered according to proximity to the paleoshoreline, with more distal sections on the right and more proximal sections on the left. Locations of the individual measured sections are shown on the map in the lower-left side of the figure. (Precise locations of measured sections are indicated on Figure 6.) The sections are correlated using the lowstand systems tract of the sequence. Lithologies are the same as those used in Figure 8. VPDB—Vienna Peedee belemnite; HST—highstand systems tract; TST—transgressive systems tract; LST—lowstand systems tract; SSFs—small shelly fossils.

and archaeocyaths are present in the sandy limestone at the contact with the Khairkhan Formation (Fig. 5D). Phosphatic hardgrounds and lag deposits with coated phosphate grains, small shelly fossils, and archaeocyaths are also present in other sections nearby in this area. The top of the section is marked by a transgression into hundreds of meters of thinly bedded sandstone and brown siltstone (Figs. 5G and 5H).

In the other measured section in this area (E1340), archaeocyath reefs are interbedded with tens of meters of cobble to boulder conglomerate. The conglomerate beds are well sorted with rounded clasts of sandstone and granite to very poorly sorted with angular carbonate and sandstone clasts. Clasts of almost all of the underlying Neoproterozoic to Cambrian units were found, and we suggest these conglomerate beds mark a regional unconformity. The archaeocyath reefs in the section are 1–3 m in scale and pinch out to the east. This section does not have a top contact because the section is exposed in a shallowly dipping syncline.

In the area south of the Khukh-Davaa Pass, many facies of the Khairkhan Formation are present, ranging from siltstone to sandstone to conglomerate. In some conglomeratic facies, limestone archaeocyath-rich clasts of the Salaagol Formation are dominant, but in other facies, they are absent. In the most southern part of Figure 6D, the Khairkhan Formation contains building-size limestone olistoliths that are visible in satellite imagery. The upper part of the Khairkhan Formation consists of light-green, gray, brown, and black finely laminated siltstone (Figs. 5G and 9C). The thickness of the formation is difficult to determine due to faulting, folding, lateral facies change, and poor exposure of the upper Khairkhan Formation, but in this area, it is hundreds of meters thick.

Overlying the Khairkhan Formation in the area just south of the Khukh-Davaa Pass (Figs. 1D and 6D), there is a buff- to red-colored, variably silicified microbial dolostone of unknown age (Fig. 5I). This unit is also present in the section southeast of Taishir and near Kvetee Tsakhir Nuruu. The contact between the Khairkhan Formation and this chert unit was not exposed in any of the localities included in this study.

Salaa Gorge and Tsagaan Gorge (F874, D718, D720, F1131, E1109)

These two gorges are ~4 km away from each other on the northern flank of the Khevtee Tsakhir Range, with Tsagaan Gorge being the eastern of the two (Fig. 6E). They are ~20 km southwest of the village of Jargalant. Khomentovsky and Gibsher (1996) mapped a thrust repetition in the lower part of the Bayangol Formation; however, we saw no evidence for a major thrust repetition and instead mapped this area as having a number of right-lateral faults. Unfortunately, there is no exposure between Tsagaan Gorge and the exposure to the NW, close to where section D720 was measured, which obscures some of the fault traces in the lower Bayangol Formation. Because this area was more structurally complex than was previously suggested (Khomentovsky and Gibsher, 1996) and there was uncertainty in the nature and offset of some of the faults, we did not measure or sample the middle Bayangol at high resolution.

The Tsagaan Gorge section of the Zuun-Arts Formation was previously measured, described, and sampled by Voronin et al. (1982), Gibsher and Khomentovsky (1990), Brasier et al. (1996b), and Khomentovsky and Gibsher (1996). These studies failed to note that the upper-middle part of the section is faulted and recrystallized, obscuring bedding and sedimentary features. This portion of the strata was not measured or sampled, and as a result, the thickness of the Zuun-Arts Formation at this locality is uncertain. The unmeasured portion is marked by a fault in Figure 7. The basal Bayangol Formation was measured between Tsagaan and Salaa Gorges.

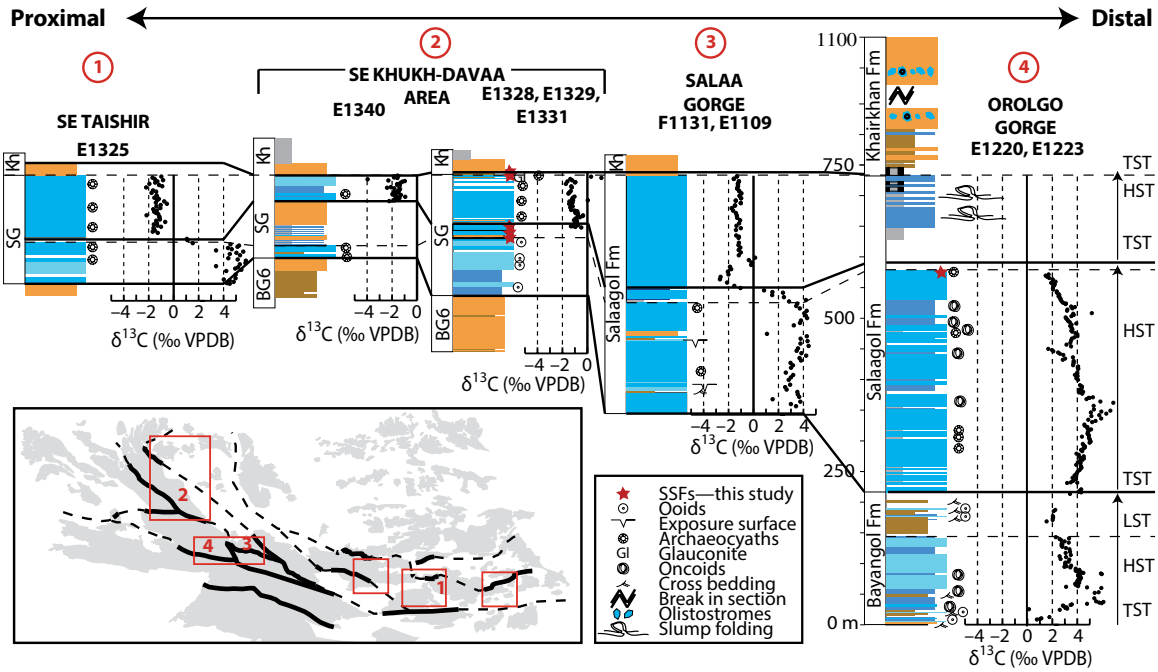

Figure 9. (A) Autochthonous to allochthonous thrust sheets of different facies of the Khairkhan Formation and cumulate ultramafics and serpentinite. Clasts of ultramafic rock have been found in the Khairkhan Formation. Together, these stratigraphic and sedimentological results support the claim that the Zavkhan Basin was a foreland basin (Macdonald et al., 2009). (B) Photo of the cumulative ultramafics in thrust contact with the Salaagol Formation in northern Orolgo Gorge. (C) Photo of the parautochthonous facies of the Khairkhan Formation from SE Khukh-Davaa area.

The sedimentology, paleontology, and paleoenvironment of the Salaagol Formation at Salaa Gorge have been described in detail by Kruse et al. (1996). We remeasured this section to use the detailed sedimentology and paleontology of previous workers as a reference point, and also to sample the entire formation at a higher resolution (~4 m) for $\delta^{13}C$ chemostratigraphy. The total measured thickness of the composite section at this locality is 380 m. A red to yellow carbonaceous silt was used to tie sections F1131 and E1109 together. Figure 5B shows the upper half of the measured section (E1109) overlain by the Khairkhan Formation.

NE Khukh-Davaa (E1211, E1212)

A nearly complete, well-exposed section of the Bayangol Formation was found north of Khukh-Davaa Pass and northeast of a major NW-SE–trending fault, which faults the Ediacaran-Cambrian strata against the Zavkhan Formation (Fig. 6D). The total thickness of the Bayangol Formation at this locality is 765 m but lacks a top contact with the Salaagol Formation. The base of the section is marked by the contact between a cross-bedded ooid grainstone of the Zuun-Arts Formation and red to green phosphatic shale of the basal Bayangol Formation.

In present-day coordinates, this section is closest to E1207, a section just north of Khukh-Davaa Pass; however, these sections are separated by a major fault and, as a result, have different facies. The overall thicknesses for the different members of the Bayangol Formation are relatively similar, but the carbonate content and rock type within each of the members differ. For example, BG3 is expanded in both of these sections; however, it is more carbonate-dominated in section E1207 than it is in this one. At this locality, on the other hand, BG4 is more carbonate-dominated and thicker. The limestone capping this member was difficult to measure and sample because the terrain is very steep and massive weathering, making it difficult to see bedding and sedimentary textures. Member BG5, consisting of poorly sorted fine to very coarse sandstone, is only 87 m thick here, which is relatively thin compared to other localities. The top of the section is marked by what appear to be massively recrystallized white to pink limestone stromatolites that are likely still part of the upper Bayangol Formation. The top of this measured section is faulted against a Paleozoic intrusion.

Khunkher Gorge (E1138)

This previously undescribed section of the Zuun-Arts Formation through Bayangol Formation was measured in Khunkher Gorge and on the ridge to the west of the gorge. There are no major structural complications of the Zuun-Arts and Bayangol Formations at Khunkher Gorge, so no detailed map is presented herein, but the location is shown in Figure 1D.

The Zuun-Arts Formation was thickest at this locality. Sedimentologically, it resembles the Zuun-Arts sections in SE Khukh-Davaa. The Bayangol Formation has a basal contact with the Zuun-Arts Formation ooid grainstone and an upper contact with the Salaagol Formation. The upper contact is not shown in Figure 7 because there could be minor faulting at the base of the Salaagol Formation. Similar to other sections, members BG2 and BG3 are siliciclastic successions capped by thick limestone units. However, member BG4 is either much thicker or is much more siliciclastic-dominated in this section. The upper part of the section has abundant beds with ooids, coated grains, and oncoids. The thick oncolite bed near the top of the section looks very similar to the oncolite bed in Salaa Gorge.

Orolgo Gorge (E1220, E1223)

Insidious minor faulting is present throughout this section; however, the predictability of the conjugate fault sets, the excellent exposure, and the numerous distinct marker beds allow for tractable geological mapping, a detailed measured section, and high-resolution sampling. Our mapping in Orolgo Gorge shows that the uppermost Zuun-Arts Formation is faulted against the Taishir Formation (Fig. 6E); nowhere in this gorge is the lower to middle Zuun-Arts Formation exposed. This finding is important for small shelly fossil biostratigraphy because the FAD of *Anabarites trisulcatus* and *Cambrotubulus decurvatus* is reported from the base of the Zuun-Arts Formation at this locality, most likely because the phosphatic shale at the base of the Bayangol Formation was mistaken as the phosphatic shale at the base of the Zuun-Arts Formation (Endonzhamts and Lkhasuren, 1988). As a result of our revised geologic map, we place this small shelly fossil horizon 200–300 m stratigraphically higher, in the base of the Bayangol Formation.

Small shelly fossil horizons had been previously described at Orolgo Gorge, but no measured section or chemostratigraphy has been reported from this locality. The Bayangol, Salaagol, and Khairkhan Formations are particularly well exposed, expanded, and carbonate-dominated in this section, and geologic mapping allowed for detailed lithostratigraphic and chemostratigraphic studies in this gorge.

The measured section in Orolgo Gorge is the thickest, most carbonate-dominated section that was measured of the Bayangol Formation. In modern coordinates, it is close to Salaa Gorge; however, the two are separated by a major fault, and this section restores to the east. The exposure in the creek is excellent, but abundant minor conjugate fault sets had to be mapped in detail before measuring this section (Fig. 6E). The section has both a basal contact with the Zuun-Arts Formation and a top contact with the Salaagol Formation.

Similar to other sections, the base of the Bayangol Formation at this locality is marked by cross-bedded ooid grainstone sharply overlain by phosphatic green shale with nodular limestone. The basal ~155 m of this section are sedimentologically different from other measured sections. It is characterized by very thinly bedded (0.5–5 cm) gray to tan limestone that is often interbedded with black shale. Horizons containing small shelly fossils are abundant. At 137.5 m above the basal contact, there is a lenticular phosphatic hardground overlain by 10 cm of phosphatized ooids (Fig. 3G). Above this distinct marker bed, the limestone beds are thicker, and no additional small shelly fossil horizons were found for hundreds of meters. Above the thick, resistant limestone unit in the middle of BG2, there is ~70 m of nonexposure in the creek. Above this covered interval, there is a green bioturbated siltstone and fine-grained sandstone that contains slump folds and some fault repetitions.

Although BG2 is expanded at this locality, BG3 is condensed. However, it is similar to other sections in that there are thick limestone units in the lower-middle part of the member. One distinctive feature of BG4 is the basal portion, which is characterized by red and green shale interbedded with pink thrombolites and limestone microbialaminites. A thick microbial limestone ridge-former caps member BG4. Member BG5 is perhaps the most unusual part of this measured section because it has far more limestone beds than any other measured section in the basin. The base of BG5 is characterized by fine to very coarse, planar to cross-bedded sandstone. There is a distinct microbialaminite and microbial balls in the middle of the siliciclastics. The top of BG5 is characterized by abundant, channelized cross-bedded calcarenites, oolites, and oncolites interbedded with cross-bedded sandstone. Above the carbonate-dominated portion of BG5, there are more coarse to very coarse cross-bedded quartzarenites and calcarenites. The top contact with the Salaagol Formation is marked by red to gray silty limestone microbial reefs with dispersed archaeocyaths.

The section of the Salaagol Formation measured here (top of E1220) is a continuation of the section of the Bayangol Formation from this locality. The upper part of the Bayangol Formation has thick limestone units that are not present in other sections. As a result, the boundary between the Bayangol and Salaagol Formations

was difficult to determine. Here, we define the base of the Salaagol Formation as the base of the last major carbonate unit that is stratigraphically below the Khairkhan Formation. The base of this section is marked by a distinct red siltstone and silty microbial limestone (Fig. 5A).

The Salaagol Formation in this gorge is over 343 m thick. The top of the formation is a talus slope and is not exposed on either side of the gorge. The basal to middle part of the formation is predominantly gray to pink to green limestone microbialites with siltstone interbeds. The first archaeocyaths appear 70 m above the basal contact. The middle to upper portion of the section continues to be dominated by microbialites, but thinly bedded nodular limestone beds and oncolites become increasingly more common in the upper part of the section.

The overlying Khairkhan Formation is folded in a syncline at this locality. The formation was not measured in detail but was instead just generally characterized on an overturned limb on the north side of the fold (Fig. 6E). The estimated thickness of the formation here is ~550 m. The basal part of the formation contains limestone boulders and olistoliths that are concordant to the surrounding matrix of shale and silt, and slumping. The rest of the formation is dominated by sequences of very poorly sorted, matrix-supported conglomerate with angular clasts of black chert, quartz, ultramafics, and limestone (Figs. 5E and 5H) that fine up to sandstone and siltstone. Many of conglomerates and coarse sandstone are channelized. Some of the conglomerates contain larger boulders and olistoliths of archaeocyath-rich limestone. To the north and west of this section, there are building-size olistoliths of the Salaagol Formation in the Khairkhan Formation (Fig. 5F). The contact between the Salaagol and Khairkhan Formations is not well exposed in this gorge; however, samples with phosphatized archaeocyaths and small shelly fossils (similar to those in Fig. 5A) were discovered in a talus slope near the contact.

The Khairkhan and Salaagol Formations are in fault contact with ultramafic cumulates and serpentinite (Fig. 7B), and in the area to the north and west of Orolgo Gorge, the Khairkhan Formation contains clasts of the ultramafic rocks (Fig. 6E). Northwest of the ultramafic rocks in Orolgo Gorge and on the northeastern edge of the large Paleozoic intrusion, there are hundreds of meters of very finely laminated green to white to brown siltstone of the Khairkhan Formation (Figs. 5G, 9A, and 9C). Due to the poor exposure and the nearby intrusion, the nature of the underlying contact is not clear; however, the map relation with the underlying olistolith facies of the Khairkhan Formation suggests that it is a fault contact (Fig. 9A).

Small Shelly Fossil Biostratigraphy

We place previously reported small shelly fossil horizons (Korobov and Missarzhevsky, 1977; Voronin et al., 1982; Endonzhamts and Lkhasuren, 1988; Zhegallo and Zhuravlev, 1991; Goldring and Jensen, 1996; Khomentovsky and Gibsher, 1996) into the new stratigraphic and $\delta^{13}C$ chemostratigraphic context, and we document new small shelly fossil horizons in multiple sections from across the Zavkhan terrane. Here, we present changes in the results of stratigraphic placement of previously described small shelly fossil horizons and the resulting revised FADs as a result of new geologic mapping and refined correlations.

The lowermost small shelly fossil finds on the Zavkhan terrane are reported from the Zuun-Arts Formation in three localities: Kvetee Tsakhir Nuruu (Dorjnamjaa et al., 1993), Orolgo Gorge, and Salaa Gorge (Endonzhamts and Lkhasuren, 1988). Dorjnamjaa et al. (1993) reported *Anabarites trisulcatus* from siliceous phosphorite at the base of the Zuun-Arts Formation; however, other workers were not able to confirm this finding (Brasier et al., 1996b). After extensive searching near the base of the Zuun-Arts Formation at this locality, we were not able to find any small shelly fossil horizons, and we suspect that the siliceous phosphatic horizon at the base of the Bayangol Formation was confused for the one at the base of the Zuun-Arts Formation.

Similarly, the FADs of *Anabarites trisulcatus* and *Cambrotubulus decurvatus* from the base of the Zuun-Arts Formation in Orolgo and Salaa Gorges could not be confirmed (Endonzhamts and Lkhasuren, 1988). In fact, in Orolgo Gorge, the Zuun-Arts Formation is faulted against the Taishir Formation, and only the uppermost part of the former is present (Fig. 6E). Again, we suspect that confusion between the two phosphatic horizons resulted in the misplacement of this important FAD. These revisions are shown in Figure 7.

Using the locations of previously published small shelly fossil horizons from Bayan Gorge (Khomentovsky and Gibsher, 1996) and our revised mapping, some of the small shelly fossil horizons (R-IV through R-X; see Fig. 7) have been moved stratigraphically up into member BG3. The previous interpretation was the result of incorrect mapping of BG3 as a thrust repetition of BG2 (Khomentovsky and Gibsher, 1996).

The small shelly fossil horizons from the Taishir section had not been put into stratigraphic context because the area had neither a detailed map nor a composite measured section. With our revised mapping and composite measured section, we place the previously reported small shelly fossil horizon in the upper part of member BG3 (see Fig. 7).

New small shelly fossil horizons are reported here, but the phosphatized small shelly fossils within them have not yet been dissolved, identified, or imaged. The small shelly fossil horizons are almost always preserved as lenticular lag deposits that pinch in and out laterally (Fig. 3G). They are often found in association with phosphatized coated grains and ooids. One exception to this is the type of preservation seen in the small shelly fossil horizons in the basal part of Orolgo Gorge, where the small shelly fossils are large, unbroken, and not found in association with other grains (Fig. 3H). Additionally, they are found on dozens of bedding planes in the basal ~200 m of measured section E1220. More generally, the small shelly fossil horizons are not discrete beds that are continuous markers across the basin, but they rather occur at different stratigraphic horizons in different sections, consistent with the rapid lateral facies changes across the basin.

Ichnofossil Biostratigraphy

Abundant and diverse trace fossils are present throughout the Bayangol Formation, and as Goldring and Jensen (1996) pointed out, western Mongolia is one of the few places globally in which they are interbedded with skeletal fossil assemblages, providing the opportunity to calibrate the relative timing of these two types of fossil records. Here, we present a few more notable finds to add to the well-documented ichnotaxa that have been previously described and adjust their stratigraphic placement.

Given that the Precambrian-Cambrian boundary is defined as occurring at the FAD of the trace fossil *T. pedum* at the Fortune Head section (Landing, 1994), ichnologists working in the Zavkhan terrane have devoted much time and energy trying to document the FAD of this trace fossil. The FAD of this fossil, according to Goldring and Jensen (1996), is in unit 20 of the Bayangol Formation. With our revised geological mapping and stratigraphy (see previous results sections "Geological Mapping" and "Description of Key Sections"), we place this unit at the contact between members BG3 and BG4 (see Fig. 7). Other ichnogenera from unit 20 include *Monomorphichnus* isp., *Hormosiroidea* isp., and *Rusophycus* cf. *avalonensis* (Goldring and Jensen, 1996). Just below, in unit 18, or what we interpret as the lower part of member BG3, *Helminthoida*, *Spatangopsis*, and *Nemiana* were found. The trace fossil assemblage from member BG4 at Taishir includes *Oldhamia*, *Plagiogmus*, and possible *Zoophycus* (Fig. 7; Goldring and Jensen, 1996).

We emphasize that the preservation of *T. pedum* and the other trace fossils is highly facies dependent in the Zavkhan terrane. Although we were not extensively searching for *T. pedum*, we did not find it at any other stratigraphic horizon or in any other measured section. We agree with previous workers that placing the Precambrian-Cambrian boundary at the FAD of *T. pedum* on the Zavkhan terrane contradicts other lines of evidence that suggest that the Precambrian-Cambrian boundary is actually much lower in the stratigraphy. Although some workers have shown that there is a wide environmental tolerance for *T. pedum* and have used this to argue for further support of the GSSP type section of the Precambrian-Cambrian boundary (Buatois et al., 2013), many other workers have shown trace fossil production and preservation of *T. pedum* to be strongly lithofacies controlled (Geyer and Uchman, 1995; MacNaughton and Narbonne, 1999; Gehling et al., 2001; Geyer, 2005). As a result, using *T. pedum* as a global chronostratigraphic marker has been problematic on most Cambrian paleocontinents, notably in Siberia, China, Mongolia, and Kazakhstan (Babcock et al., 2011, 2014; Landing et al., 2013).

Although *T. pedum* was extremely difficult to find in the Zavkhan terrane, there were many sandstone horizons that yielded abundant and diverse trace fossils. Figures 3I, 3J, 3K, and 3L display a few of the exceptional ichnofossils that were found in the Khunkher and Bayan Gorges. The early arthropod trace fossils in Figures 3I and 3J are from middle BG3 and that in Figure 3K is from BG5 in the Khunkher section (for exact horizons, see Fig. 7). The trace fossil in Figure 3L is from BG5 in Bayan Gorge.

Carbon Isotope Chemostratigraphy

Carbon isotope ($\delta^{13}C$) chemostratigraphy for individual sections of the Zuun-Arts and Bayangol Formations and for the Salaagol Formation for each locality is presented in Figures 7 and 8, respectively. The $\delta^{13}C$ values from seven measured sections of the Zuun-Arts Formation are presented here. The top of the Zuun-Arts Formation is marked by at least one large negative excursion that has a minimum of ~–7‰. This excursion was recognized by previous workers (referred to as anomaly "W"), and it has been correlated globally with the negative $\delta^{13}C$ excursion that, despite some uncertainty in precise correlations (or summary, see Babcock et al., 2014 f), has been found in association with the FAD of *T. pedum* (Narbonne et al., 1994; Brasier et al., 1996b; Corsetti and Hagadorn, 2000).

The $\delta^{13}C$ values from nine measured sections of the Bayangol Formation are presented here. Brasier et al. (1996b) identified positive excursions B–F in the Bayangol Formation, and data presented here confirm the existence of at least five positive excursions. All measured sections presented here show high-frequency oscillations in $\delta^{13}C$ values that range between ~–6‰ and +6‰. Interestingly, the positive excursions are sharp and pronounced, whereas the negative excursions have less-pronounced minimum values. The limestone beds in BG5 from Orolgo, Bayan, and Khunkher Gorges, the three gorges that have exposure of carbonates in the upper Bayangol Formation, have unusually high $\delta^{13}C$ values of <+6‰.

The $\delta^{13}C$ profiles for the Salaagol Formation were surprisingly different from the previously reported $\delta^{13}C$ values from Salaa Gorge and Zuun-Arts Ridge (Brasier et al., 1996b). In Orolgo Gorge, the $\delta^{13}C$ values are as high as 7‰. In Salaa Gorge and in SE Taishir, the $\delta^{13}C$ values in the lower-middle part of the section reach ~+4.5‰. The $\delta^{13}C$ values in the upper part of the measured sections at Salaa Gorge, Khukh-Davaa, and SE Taishir drop to ~–2‰ to –1‰. Brasier et al. (1996b) reported 23 $\delta^{13}C$ values that range between –0.6‰ and –1.6‰ from 44 m of strata of the Salaagol Formation at the Zuun-Arts locality and $\delta^{13}C$ values that range between –0.2‰ and –1.2‰ from 22 samples from the upper 117 m of the Salaagol Formation at Salaa Gorge. The discrepancy between the range of $\delta^{13}C$ values reported here and previously reported values is the result of earlier workers only sampling the upper portions of the Salaagol Formation.

DISCUSSION

Facies Model and Sequence Stratigraphy

Within the Zuun-Arts through Khairkhan succession, there are several major sequence boundaries that can be used as stratigraphic tie lines across the basin. The phosphatic shale units at the bases of the Zuun-Arts and Bayangol Formations vary in thickness and color but are easily recognizable stratigraphic markers of transgressions in the sequence. The phosphatic shale at the base of the Bayangol Formation is a distinct stratigraphic marker that we use as the datum upon which to align the sections in Figure 7. The sequence boundaries with the Bayangol Formation are discussed in detail. The top contact of the Salaagol Formation with the Khairkhan Formation is marked by a LST overlain by a sharp transgression that, in some sections, is marked by a phosphatic hardground overlain by phosphatized small shelly fossils, archaeocyaths, and coated grains. In many sections, this contact is faulted, perhaps because the contact represents a sharp rheologic boundary between a massive limestone reef and more fissile mixed siliciclastic units. Nonetheless, there are many sections that are well preserved and not compromised by faulting for which the transgression can be used as the datum for the sections in Figure 8.

The tie lines in Figures 7 and 8 show how the measured sections in the Zavkhan terrane correlate to one another using major sequence boundaries within the Bayangol and Salaagol Formations. Portions of the major sequences within the Bayangol Formation are also shown and annotated in photographs from portions of the sections in N Khukh-Davaa Pass and S Bayan Gorge in Figure 4. Generally, the massive carbonate reefs that cap each informal member of the Bayangol Formation represent the HST of the sequences, with the maximum flooding surface (MFS) near the base of each of these. These are in turn overlain by medium to coarse sands that represent the LST of the sequences. The thicknesses of the LSTs and TSTs vary between sections, depending on a section's proximity to the shoreline. The more distal sections tend to preserve thinner LSTs and thicker TSTs than the more proximal ones.

Complicating the identification of major sequence system tracts are minor shallowing-up sequences within the large sequences as well as bypass channel sands. Obvious examples of bypass channel sands are in members BG4 and BG5 of the Khunkher Gorge section (Fig. 10). The nearby sections contain ~150-m-thick limestone reefs capping BG4 and BG5, whereas the section in Khunkher Gorge instead has relatively thin limestone units with abundant oncolite, ooid, and calcarenite beds at the same stratigraphic horizon. The $\delta^{13}C$ chemostratigraphic curves provide independent confirmation that the lithologically different units of BG4 and BG5 in the Orolgo and Khunkher Gorges were being deposited synchronously.

One interesting feature of the integrated chemostratigraphy and sequence stratigraphy is that the large $\delta^{13}C$ excursions of the Bayangol Formation generally seem to occur at the same frequency as the major sequence boundaries. With sedimentological, stratigraphic, and chemostratigraphic data from across the basin, mechanistic hypotheses about the relationships between feedbacks in sea level, associated nutrient input, and the carbon cycle can begin to be tested with data from the rock record. The negative $\delta^{13}C$ excursions rarely coincide with major sequence boundaries, but the pronounced positive $\delta^{13}C$ excursions are often found preserved between the TST and the HST of the sequences.

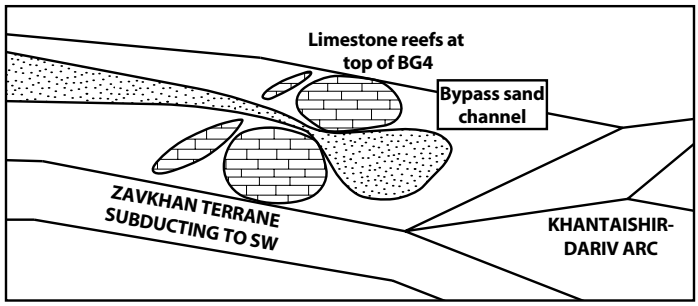

Figure 10. Schematic depositional model for member BG4 of the Bayangol Formation. Evidence for bypass channel sands exists in the measured section of the upper Bayangol Formation in Khunkher Gorge (Fig. 7).

Using the age model presented herein and the resulting estimates for sedimentation rates, we calculated the lag time between transgressions and positive $\delta^{13}C$ excursions.

An important tectonic result of the new facies model for the Zavkhan terrane is the documentation of the deep-water, allochthonous facies of the Khairkhan Formation in northern Orolgo Gorge (Fig. 9A). These include poorly sorted conglomeratic facies of the Khairkhan Formation that contain ultramafic clasts. Nearby, the Khairkhan and Salaagol Formations are in thrust contact with a large ultramafic body (Figs. 6E and 9B). The second deep-water facies of the Khairkhan Formation is hundreds of meters of very finely laminated siltstone in the area just to the north of Orolgo Gorge (Figs. 9A and 9C). We suggest that the deeper-water facies of the Khairkhan Formation are allochthonous to the Zavkhan terrane, bolstering the stratigraphic argument that the late Ediacaran to early Cambrian strata were deposited in a foreland basin (Macdonald et al., 2009). Thus, although small-scale transgressions associated with positive $\delta^{13}C$ excursions may be global and eustatic, the larger-scale sequences and basin architecture are undoubtedly the product of local tectonism.

Constructing a Composite Carbon Isotope Curve for the Zavkhan Terrane

The $\delta^{13}C$ chemostratigraphic data are generally consistent with the sequence stratigraphic correlations used in Figures 7 and 8. In Figure 11, the composite curve is presented next to the $\delta^{13}C$ curve from Orolgo Gorge, the most expanded, carbonate-dominated section in the Zavkhan terrane in which 2p–6p are preserved. Details regarding the specific tie points used in each of the late Ediacaran to early Cambrian Mongolian formations are discussed in stratigraphic order. The specific $\delta^{13}C$ values that were used as tie points between sections in the Zavkhan terrane are in the supplementary material.[1]

Although high-resolution $\delta^{13}C$ chemostratigraphic correlation within the Zuun-Arts Formation is complicated by high-frequency variability in the lower half of the formation, there is one large negative excursion that is <9.5‰ in magnitude preserved near the top of all measured sections of the Zuun-Arts Formation. The more proximal sections (Taishir and Kvetee Tsakhir Nuruu) preserve a negative $\delta^{13}C$ excursion in the middle of the formation. The lateral variability within the Zuun-Arts Formation is the result of diachronous deposition. The two phosphatic shales that bookend the formation mark two transgressions that represent two synchronous sequence boundaries across the Zavkhan terrane. Using this sedimentological and sequence stratigraphic argument, the upper part of the Zuun-Arts Formation in the proximal sections cannot be correlative with the lower Bayangol Formation in the more distal sections.

Correlations between the nine measured sections of the Bayangol Formation are not as straightforward as those in the Zuun-Arts and Salaagol Formations for three reasons: (1) Unlike the other two formations, there is not continuous carbonate deposition in the Bayangol Formation, (2) there are large lateral changes in facies and bed thickness across the basin that are further complicated by sandstone-filled bypass channels, and (3) the carbon cycle rapidly oscillated during the earliest Cambrian with several excursions that, taken alone, are nondistinct. To further complicate correlations, compared to the very smooth $\delta^{13}C$ profile with five clear positive excursions from Sukharikha, Siberia (Kouchinsky et al., 2007), the sections of the Bayangol Formation preserve additional minor excursions (Fig. 7).

The magnitude of the positive excursions as well as the thicknesses over which they occur vary between the sections. It is also clear from comparing both the lithostratigraphy and chemostratigraphy between measured sections that the facies transitions are diachronous across the basin. This interpretation is supported by comparing the sections from Khunkher and Orolgo Gorges (Fig. 7); the chemostratigraphic profiles for the upper parts of the Bayangol Formation are almost identical, but the lithostratigraphy is very different. There is also obvious diachroneity between the two measured sections near Khukh-Davaa Pass, with the chemostratigraphic profiles closely matching each other but with noticeable differences in the lithostratigraphy. These are just two of many obvious examples of the lithological variability of the sections of the Bayangol Formation, highlighting the importance of the integrated approach used here.

One interesting chemostratigraphic feature is the positive excursion (~7‰) at the base of the measured section at Orolgo Gorge. Sedimentologically, the basal part of this section looks very different from any other section because it contains a much thicker section of phosphatic shale, black shale, and interbedded limestone. We have interpreted this portion of the stratigraphy as an expanded basal part of the Bayangol Formation. It is important to note, however, that the sharp drop from positive to negative $\delta^{13}C$ values occurs across a sharp sedimentological contact that contains a phosphatic hardground, phosphatized ooids, and pyrite pseudomorphs (Fig. 3G). We have interpreted this as a small unconformity in the succession.

Compared to the correlations within the lower formations, sequence and chemostratigraphic correlations between sections of the Salaagol Formation (Fig. 8) are relatively straightforward. Comparison of the sedimentology and chemostratigraphy between sections demonstrates that there is diachronous deposition of this formation and large facies changes across the basin. This interpretation is supported by comparing parts of the formation between the sections at Orolgo (E1220) and Salaa Gorge (F1131 and E1109). The section at Orolgo Gorge is much more expanded with abundant oncolite beds. Also of note are $\delta^{13}C$ values, which jump from positive to negative across a sequence boundary in the Salaagol Formation. The details and age model implications of this change in $\delta^{13}C$ values are discussed later herein.

[1]GSA Data Repository item 2015265, stratigraphic, chemostratigraphic, biostratigraphic, and chronostratigraphic data presented in this paper, is available at http://www.geosociety.org/pubs/ft2015.htm or by request to editing@geosociety.org.

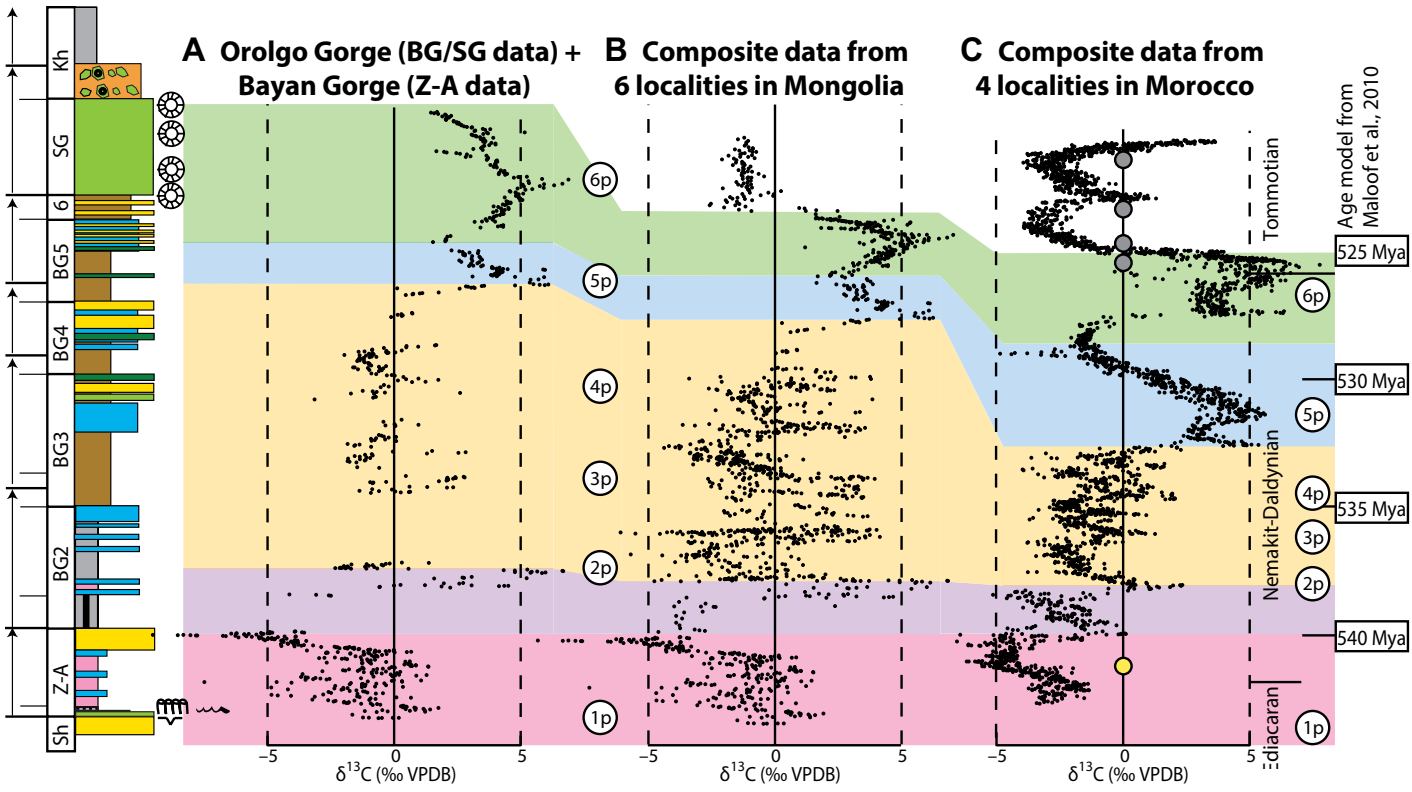

Figure 11. Revised $\delta^{13}C$ chemostratigraphic age model for the Zuun-Arts through Salaagol Formations in the Zavkhan terrane. (A) $\delta^{13}C$ isotopes plotted next to a generalized stratigraphic column for the Zuun-Arts Formation at Bayan Gorge and the Bayangol through Khairkhan Formations at Orolgo Gorge. Here, $\delta^{13}C$ values are plotted against measured thickness. These data are plotted because Orolgo Gorge has the thickest, most carbonate-dominated section of the Bayangol and Salaagol Formations. (B) A composite $\delta^{13}C$ curve of six sections from the Zavkhan terrane. Generally, sections are correlated using sequence stratigraphy, and here, the composite curve is constructed by using positive $\delta^{13}C$ excursions for tie points and stretching the $\delta^{13}C$ curves between. The uppermost Salaagol and Khairkhan Formations are Tommotian in age. (C) A composite $\delta^{13}C$ curve from four localities in Morocco, a locality where there are absolute age constraints (Maloof et al., 2005, 2010b). Here, $\delta^{13}C$ values are plotted against age. U/Pb tie points are marked by yellow (Oman—Bowring et al., 2007) and gray (Maloof et al., 2005, 2010a) circles. The age model on the right side of the figure is from Maloof et al. (2010a). The transparent colored boxes show how these three $\delta^{13}C$ chemostratigraphic curves correlate to each other. Following Maloof et al. (2010a), positive excursions in the late Ediacaran through Nemakit-Daldynian are numbered and labeled with white circles. VPDB—Vienna Peedee belemnite; HST—highstand systems tract; TST—transgressive systems tract; LST—lowstand systems tract.

Refined Age Model

Carbon isotope chemostratigraphy is useful as both a correlation tool and, with the absence of absolute ages, for constructing a more precise age model that can be used to correlate between the composite $\delta^{13}C$ curve from the Zavkhan terrane and other sections globally that do contain absolute ages. Additionally, under the assumption that changes in $\delta^{13}C$ values mark synchronous, global markers, chemostratigraphic correlation avoids circular arguments that result from correlating poorly established, facies-dependent, and highly regional paleontological biozones.

We correlate the largest negative $\delta^{13}C$ excursion at the top of the Zuun-Arts Formation with other negative $\delta^{13}C$ excursions that have been documented globally near the Ediacaran-Cambrian boundary in localities such as Morocco, China, Siberia, Oman, the western United States, and northwestern Canada (Narbonne et al., 1994; Corsetti and Hagadorn, 2000; Maloof et al., 2005; Kouchinsky et al., 2007; Li et al., 2009). This negative excursion at the Ediacaran-Cambrian boundary, the high-frequency oscillations during the Nemakit-Daldynian, and the two very high excursions at the end of the Nemakit-Daldynian and in the early Tommotian (Maloof et al., 2005, 2010b; Kouchinsky et al., 2007), are all present in the Zavkhan terrane strata, increasing confidence in the use of $\delta^{13}C$ chemostratigraphic profiles as a tool for global correlation.

Here, we map late Ediacaran and early Cambrian records of $\delta^{13}C$ variability from Mongolia onto the Moroccan $\delta^{13}C$ record, which is constrained with absolute U/Pb ages from Morocco (Maloof et al., 2005, 2010b) and Oman (Bowring et al., 2007). Although Morocco lacks fossils in the earliest Cambrian, it has a very expanded $\delta^{13}C$ curve from four localities with four chemical abrasion–isotope dissolution–thermal ionization mass spectrometry (CA-ID-TIMS) U/Pb zircon ages on ash beds of 525.343 ± 0.088 Ma (Maloof et al., 2005, 2010b), 524.837 ± 0.092 Ma (Maloof et al., 2010b), 523.17 ± 0.16 Ma (Maloof et al., 2010b), and 520.93 ± 0.14 Ma (Landing et al., 1998; Compston et al., 1992; Maloof et al., 2010b). The age from the Ediacaran-Cambrian boundary is a CA-ID-TIMS U/Pb zircon age on an ash bed from Oman dated at 541.00 ± 0.29 Ma (Bowring et al., 2007; Peng et al., 2012).

Although there is some uncertainty in precise chemostratigraphic correlation between the Mongolia and Morocco composite curves, large-scale uncertainty is mitigated by the unambiguous end-Ediacaran negative excursion and the end Nemakit-Daldynian positive excursion. High-frequency $\delta^{13}C$ oscillations during the earliest Cambrian are bookended by these two easily identifiable chemostratigraphic markers that are preserved in both Mongolia and Morocco. Following Kouchinsky et al. (2007) and Maloof et al. (2010a), we assigned the positive excursions numbers 2 through 6 (1 is the positive excursion during the end-Ediacaran). It is interesting that both in Mongolia and Morocco, there appear to be additional minor excursion between 1p and 2p, 3p and 4p, and 4p and 5p, suggesting that the carbon cycle was oscillating even more rapidly than previously thought during the earliest Cambrian.

This refined age model results in a couple of important new interpretations about the age of the strata in the Zavkhan terrane. The first is that the Bayangol Formation is entirely Nemakit-Daldynian in age, rather than extending into the Tommotian as was previously suggested. The evidence supporting this interpretation is the very high $\delta^{13}C$ values of ~7‰ near the top of the measured sections of the Bayangol Formation in Bayan, Khunkher, and Orolgo Gorges. The only two times during the early Cambrian that the $\delta^{13}C$ values were this high was during the middle to late Nemakit-Daldynian. A second important point is that there is a second very high $\delta^{13}C$ excursion that begins in the uppermost Bayangol Formation and reaches values of 8‰ in the lower Salaagol Formation. The level of peak values is most clearly documented at Orolgo Gorge, but it is reproduced in other measured sections of the Salaagol Formation as well (Figs. 7 and 8).

This second very high $\delta^{13}C$ peak coincides with the FAD of archaeocyaths in the Zavkhan terrane. Correlating this $\delta^{13}C$ excursion with the excursion at the Nemakit-Daldynian to Tommotian boundary distinguishes the archaeocyaths in the lower to middle Salaagol Formation as among the earliest documented archaeocyaths globally. The $\delta^{13}C$ values between the two high peaks in Mongolia are not as low as the –2‰ to –1‰ values in Morocco, which we interpret as representing a small unconformity in the conglomerate beds just below the base of the Salaagol Formation.

Unfortunately, the $\delta^{13}C$ values of –2‰ to 0‰ of the upper Salaagol Formation are not diagnostic of $\delta^{13}C$ values of any one member in the early Cambrian, and they are consistent with a Tommotian, Atdabanian, or a Botomian age. Here, we discuss two possible age models for the upper Salaagol Formation. The first age model is that the Salaagol Formation is Nemakit-Daldynian to Tommotian in age with relatively continuous strata. This age model is based, in part, on the similarity between Sr isotope values from Tommotian strata in Siberia (Derry et al., 1994; Kaufman et al., 1996) and from the upper Salaagol Formation (Brasier et al., 1996b). It is also based on the complete lack of any trilobite fossils (whole or disarticulated) in the upper Salaagol and Khairkhan Formations, which would be expected to occur if these units were Atdabanian or Botomian in age.

However, this age model is in conflict with the archaeocyath biostratigraphy from the Zavkhan terrane, which uses a few archaeocyath species that are thought to be diagnostic of the Atdabanian and Botomian Stages. Most of the archaeocyaths collected by Kruse et al. (1996) from the Salaagol Formation range from the Tommotian to Botomian in age; however, there are a few species, such as *Tabulacyathellus bidzhaensis*, *Archaeopharetra marginata*, *Couberticyathus lepidus*, *Robustocyathellus abundans*, *Orbicyathus mongolicus*, and *Ladaecyathus melnikovae*, that are thought to be restricted just to the Atdabanian and/or Botomian (Paleobiology Database). We emphasize that the age ranges for these specimens were calibrated in just Siberia, and thus it is possible that these specimens have a longer stratigraphic extent globally. The second age model for the Salaagol Formation, which is based on the robustness of using these few archaeocyth species for biostratigraphy, requires there to be a 6–10 m.y. unconformity in the medium sandstone to pebble conglomerate beds of the middle-upper Salaagol Formation (Fig. 8).

The second age model necessitates a multistage subsidence history in which the margin subsides for ~15 m.y., there is a hiatus for 6–10 m.y., and then it subsides again for a few million years during deposition of the upper Salaagol and Khairkhan Formations. The 6–10 m.y. hiatus in subsidence could reflect either slab breakoff or the passing of a peripheral forebulge before the final obduction of the allochthonous flysch of the Khairkhan Formation. The subsidence history for the first age model is much simpler, with a margin that is subsiding for 16–20 m.y. before the final collision of the Khantaishir-Dariv arc. With a lack of trilobites, Tommotian-like Sr values, and a simpler subsidence mechanism, we prefer the first age model for the upper Salaagol and Khairkhan Formations (Fig. 11). We suggest that the few archaeocyath species from the upper Salaagol Formation that are thought to be diagnostic of the Atdabanian or Botomian were either misidentified or have longer stratigraphic ranges than was previously thought.

Refined Biostratigraphy

By placing the previously described fossil horizons in an accurate sequence stratigraphic and chemostratigraphic framework, we can compile a new composite biostratigraphic range chart for ichnofossils and body fossils for the Zavkhan terrane (Fig. 12). Additionally, this work establishes the necessary framework for more detailed paleontological studies in new sections from across the basin.

One important result is that this work helps resolve the long-standing problem of understanding the relative timing of the FAD of *T. pedum*, the FAD of small shelly fossils, and the negative excursion that is associated with the Ediacaran-Cambrian boundary. By adhering strictly to the GSSP definition of the boundary as the horizon that coincides with the FAD of *T. pedum* (Landing, 1994), the Ediacaran-Cambrian boundary in the Zavkhan terrane would be placed between members BG3 and BG4 (Fig. 12), contradicting other lines of evidence that suggest the boundary is much lower. These lines of evidence include (1) the FAD of *T. pedum* is ~275 m above the large negative carbon isotope excursion, which has been commonly used as a secondary chronostratigraphic marker (Grotzinger et al., 1995; Brasier et al., 1996b; Maloof et al., 2005, 2010a; Zhu et al., 2006; Peng et al., 2012), in the Zuun-Arts Formation, (2) the FAD of *T. pedum* is ~250 m above the FAD of small shelly fossils, and (3) the FAD of *T. pedum* is stratigraphically above the FAD of *Rusophycus*, which inverts the normal ichnofossil biostratigraphy (Crimes, 1987, 1992; MacNaughton and Narbonne, 1999). The facies dependence and rarity of *T. pedum* in the Zavkhan terrane provide further support for reassessing the Ediacaran-Cambrian boundary with a marker that is not as facies dependent as the first evolutionary appearance of the behavior represented by *T. pedum*.

We were not able to reproduce any of the previous claims that the FAD of small shelly fossils is in the basal Zuun-Arts Formation, and we attribute the previous placement to misidentification of the phosphatic shales at the basal Bayangol Formation as those at the basal Zuun-Arts Formation. With the FAD of small shelly fossils shifted stratigraphically up into the basal Bayangol Formation, globally, the FAD of small shelly fossils and *T. pedum* only occur stratigraphically above the large negative carbon isotope excursion at the top of the Ediacaran-Cambrian boundary (Brasier et al., 1990; Knoll et al., 1995b; Zhou et al., 1997; Kouchinsky et al., 2001, 2007). The one section globally that is a possible exception to this is the section at Khorbusuonka River (Knoll et al., 1995a).

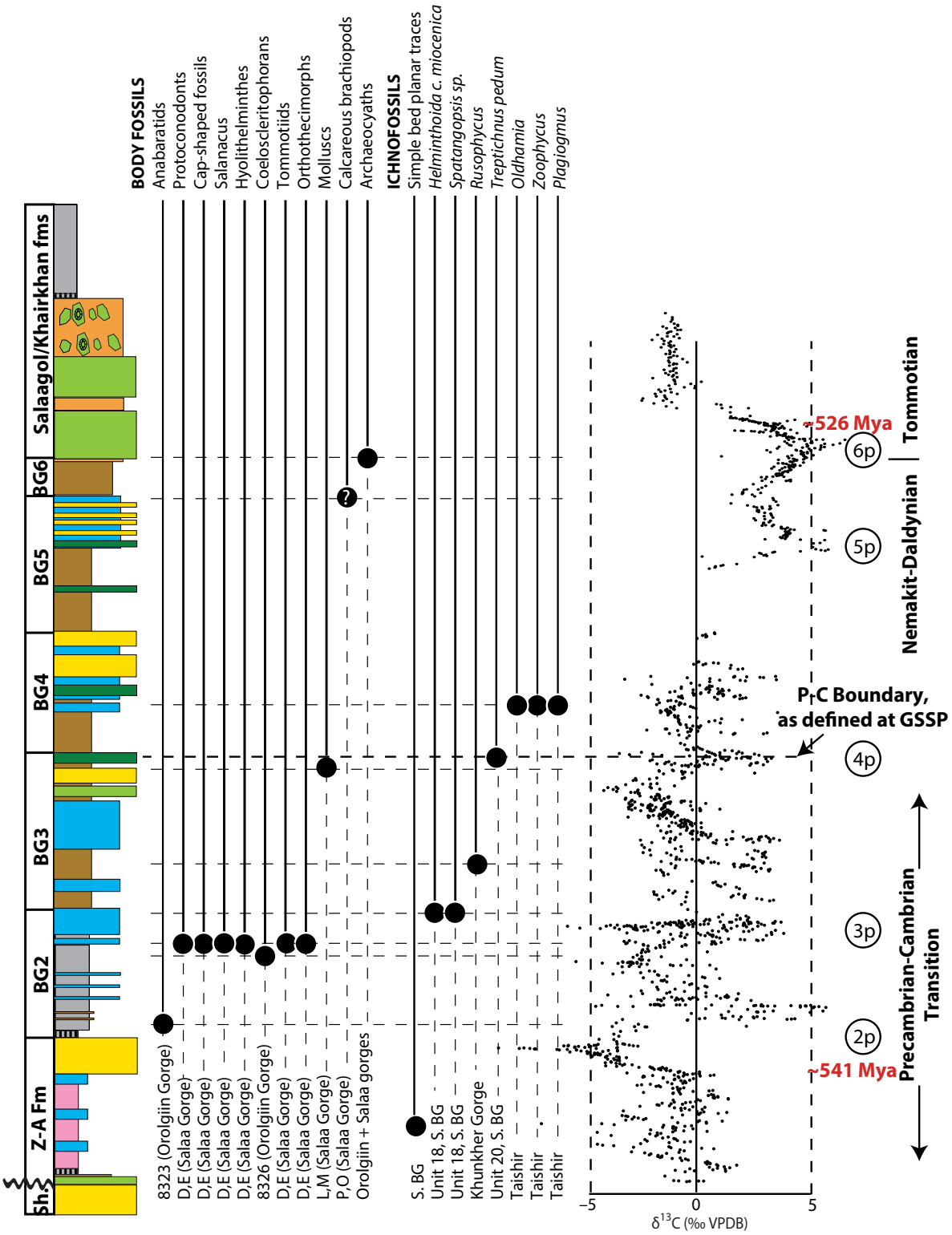

Figure 12. Composite small shelly fossil and ichnofossil biostratigraphic range chart with revised $\delta^{13}C$ chemostratigraphic age model. First appearance datums (FADs) in the fossil record are from previous workers (Korobov and Missarzhevsky, 1977; Voronin et al., 1982; Endonzhamts and Lkhasuren, 1988; Brasier et al., 1996b; Esakova and Zhegallo, 1996; Khomentovsky and Gibsher, 1996). Marker beds and section locations are listed below each circled FAD. Bold red line marks a depositional hiatus. Generic and higher group assignments used here are consistent with those from Maloof et al. (2010a, and references therein). VPDB—Vienna Peedee belemnite; GSSP—global stratotype section and point.

Many of the small shelly fossil FAD horizons in the Zavkhan terrane (tommotiids, orthothecimorphs, hyolithelminths, cap-shaped fossils, protoconodonts, *Salanacus*) are from beds "D" and "E" in the Salaa Gorge (Voronin et al., 1982; Esakova and Zhegallo, 1996). With the revised correlations and age model presented here, we place these between positive excursions 2p and 3p (Figs. 7 and 12) instead of between 1p and 2p (Maloof et al., 2010a). Other important fossils for calibrating biostratigraphic ranges globally are the molluscs *Watsonella* and *Aldanella* (Parkhaev, 2007; Steiner et al., 2007; Rozanov et al., 2008; Li et al., 2011; Parkhaev et al., 2011); however, more recently, the FADs of both taxa have been shown to be diachronous, both locally and globally (Landing et al., 2013). *Watsonella* has only been documented in one small shelly fossil horizon in the upper Bayangol Formation at Salaa Gorge, whereas *Aldanella* has not been found in the Zavkhan terrane.

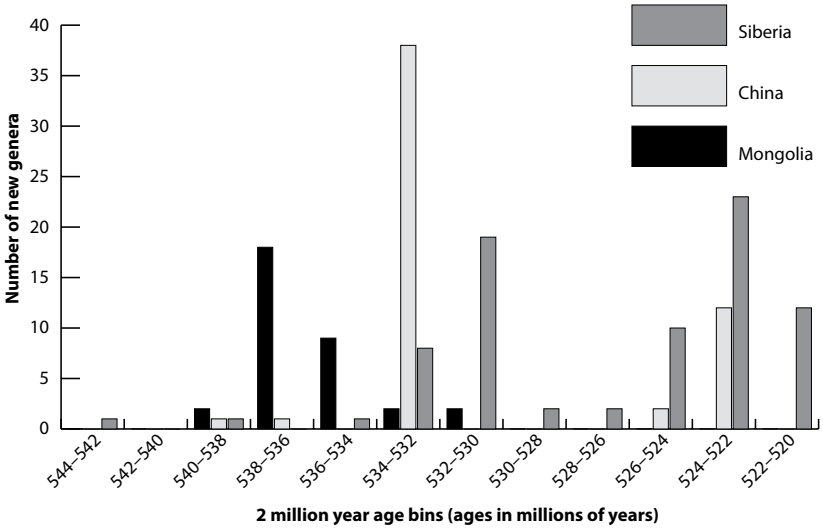

Figure 13. Number of new genera appearing in 2 m.y. time bins with revised age model from Mongolia. Data from China and Siberia are modified from Maloof et al. (2010a).

Global Origination Rates during the Earliest Cambrian

With the revised mapping, stratigraphy, and age model, we have adjusted the FADs of small shelly fossils in Mongolia. Previously, early Cambrian origination had been assessed with global FADs of small shelly fossils (Maloof et al., 2010a); however, because these compilations have been limited to three localities, namely, Siberia, China, and Mongolia, updating the age model or occurrence data for any one region causes adjustments to apparent global origination rates. Figure 13 combines the new data from Mongolia with data from China and Siberia to show the number of small shelly fossil genera that first appear globally in each time bin of 2 m.y.

The global compilation of fossil occurrence data still shows pulses of the first appearances of new genera during the earliest Cambrian. One possibility is that these peaks of fossil first appearances reflect peaks of diversification. Another possibility is that these fossil first appearance peaks instead reflect regional or global sedimentation patterns and/or taphonomic biases. The regional distribution of FADs for each peak as shown in Figure 13 demonstrates that each of the three peaks is dominated by one region. This pattern suggests that periods of deposition and the facies dependence of phosphatized fossils are the primary controllers of the FAD peaks in Figure 13. For example, in Mongolia, nearly all of the small shelly fossils are in the lower to middle Bayangol Formation, which contains phosphatic limestone beds, whereas small shelly fossils are rare in the upper Bayangol Formation, which consists almost entirely fine- to medium-grained sandstone—not the appropriate facies to preserve phosphatized small shelly fossils. This lack of appropriate facies is most likely due to the fact that these units were being deposited during the closure of the foreland basin rather than due to the closure of the phosphatization window at the end of the early Cambrian (Porter, 2004).

The second pulse of fossil FAD is due almost entirely to a huge number of FADs from China. These fossils come from the phosphatic limestone of the Zhongyicun Member. The apparent large spike in FADs in the Zhongyicun Member is due in part to three major disconformities in the strata: one at the Ediacaran-Cambrian boundary, one in the lower Dahai Member, and one at the top contact of the Dahai Member (Steiner et al., 2007). An erosional surface at the top of the Dengying Formation has been observed in the Meishucun section (He et al., 1988; Qian et al., 1996). The result is that, particularly in the southern sections of Yunnan Province, the Daibu Member and portions of the Zhongyicun Member are missing (Steiner et al., 2007). In the overlying Nemakit-Daldynian to Tommotian Upper Zhongyicun and Lower Dahai members, there are also several disconformities, erosional surfaces, and phosphatic hardgrounds, including a sub-Tommotian one in the sequence (Qian and Bengtson, 1989; Steiner et al., 2007; Yang et al., 2014), which help to explain the dearth of FADs during the late Nemakit-Daldynian. There is another major disconformity at the boundary between the Dahai Member and the overlying Shiyantou Formation. In the Meishucun section, one of the key fossil localities in this compilation, most of the Dahai Member is missing due to nondeposition or later erosion. As small shelly fossil FADs from new sections in south China continue to be added to this compilation, and as regional and global correlations continue to be refined, the pulsed pattern of global FADs will most certainly change.

Finally, in many of the fossiliferous Siberian sections, there is a sub-Tommotian unconformity (Khomentovsky and Karlova, 1993; Knoll et al., 1995b; Zhu et al., 2001). We suggest that the apparent pulses of fossil first appearances are the result of intervals of nondeposition in the sections included in this compilation and do not represent global evolutionary patterns; FADs will not be found during periods in which sediment is not deposited. Charles Darwin (1859) suggested that the apparently rapid appearance of fossils found in Cambrian strata was a product of the incompleteness in the stratigraphic record—at a smaller scale, this indeed may be the case.

Implications for Early Cambrian Carbon Isotope Variability

The large-amplitude, high-frequency excursions of inorganic $\delta^{13}C$ values that accompany the Cambrian radiation have long perplexed geologists. Brasier and Lindsay (2001) suggested that the $\delta^{13}C$ excursions are modulated by sea-level change, which, in effect, changes rates of organic carbon burial. They suggested that the positive excursions are the result of marine transgressions and the increase in the burial of organic matter, and the negative excur-

sions are the result of regressions and reduced rates of organic matter burial. Kirschvink and Raub (2003) offered an alternative methane fuse hypothesis in which the $\delta^{13}C$ excursions are attributed to the periodic release of large volumes of methane gas, which they attributed to seismic activity, sediment failure, or sediment erosion. Similarly, Maloof et al. (2005) invoked Paleocene-Eocene thermal maximum–like rapid (<100,000 yr) releases of methane or organic carbon to explain the high-frequency negative excursions in the earliest Cambrian. Squire et al. (2006) elaborated on this hypothesis by suggesting that the periodic release of methane trapped in sedimentary rocks was the consequence of rapid erosion of the Transgondwanan Supermountain. Maloof et al. (2010a) modified their earlier hypothesis for the drivers of geochemical change by stating that the rapidity and magnitude of the early Cambrian $\delta^{13}C$ excursions would require volcanic outgassing up to an order of magnitude larger than modern fluxes and a 2.25 times increase in seafloor spreading during the early Cambrian. More recently, Schrag et al. (2013) suggested that the burial of authigenic carbonate was an important sink of carbon in anoxic oceans, and that the advent of bioturbation or variations in surface redox could have resulted in fluctuations in the size of this additional carbon sink.

Coupled sequence stratigraphy and chemostratigraphy in Mongolia demonstrate that the negative $\delta^{13}C$ excursions occur predominantly in HSTs to LSTs, and the positive $\delta^{13}C$ excursions occur in TSTs to HSTs. None of the hypotheses described above provides direct explanations for a mechanistic link between eustatic sea-level change and the isotopic variations. If a weathering process is invoked, the isotopic variability indicates differential weathering of nutrients (i.e., phosphorous) that leads to organic carbon burial versus silicate weathering that in turn leads to carbonate burial. Alternatively, nutrient availability due to recycling on the continental shelf or slope might explain carbon isotope changes linked to sea level. It is also possible that authigenic carbonate may have varied with sea-level changes due to differential organic burial and anaerobic oxidation in slope sediments (Schrag et al., 2013). On the other hand, the sequence architecture in the Zavkhan terrane could have been driven by regional tectonic forces that have no bearing on the global carbon cycle. However, large-scale sequence boundaries in the Zavkhan terrane occur at roughly the same frequency as positive $\delta^{13}C$ excursions. Using the same calibration points for the positive excursions as Maloof et al. (2010a) and assuming constant rates of sedimentation between the excursions, we estimate the lag time between a maximum flooding surface and a positive excursion between the TST and HST as being between 200,000 and 500,000 yr. These rates are highly dependent on the choice of calibration points for the positive excursions, and they will continue to be refined as more early Cambrian ash horizons are dated globally. If there were high-latitude glaciers during the late Ediacaran and early Cambrian, the large-scale sequences could be consistent with Milankovitch cycles (Baode et al., 1986; Chumakov and Elston, 1989; Chumakov, 2011a; Chumakov, 2011b; Etemad-Saeed et al., 2015; Hebert et al., 2010; Meert and Van der Voo, 1994; Rice et al., 2011; Stodt et al., 2011; Torsvik et al., 1996; Zhu and Wang, 2011). Nonetheless, the repeating nature and scale of the oscillation, together with evidence of changing redox conditions (Schröder and Grotzinger, 2007; Wille et al., 2008), are suggestive of a forcing intrinsic to the carbon cycle, rather than external forcings such as volcanic or methane release.

CONCLUSION

Wide ranges of causes have been presented to explain the Cambrian radiation (review by Marshall, 2006); however, the strength of any of these explanations is limited by a precise calibration of rates of geochemical and biological change. Understanding the feedbacks between the radiation of animals and associated geochemical and environmental changes requires a precise age model and accurately calibrated fossil record. With new geological mapping, sequence stratigraphy, and a chemostratigraphic age model, we place previous small shelly fossil and ichnofossil finds into an accurate geological and temporal framework.

The new age model refines the age constraints on the Bayangol Formation to deposition entirely within the Nemakit-Daldynian. The Nemakit-Daldynian–Tommotian boundary is in the lower Salaagol Formation, coinciding with the FAD of archaeocyaths in the Zavkhan terrane. The lack of trilobite fossils and Sr isotope chemostratigraphy suggest that the middle to upper Salaagol Formation is Tommotian in age rather than Atdabanian or Botomian, as was previously suggested based on the identification of archaeocyath species with poorly constrained age ranges.

The FAD of small shelly fossils in the Zavkhan terrane is moved stratigraphically hundreds of meters up into the Bayangol Formation. With one possible exception (Knoll et al., 1995a), the FAD of small shelly fossils and the FAD of *T. pedum* globally occur above the nadir of the negative carbon isotope excursion at the base of the Cambrian. The FADs of tommotiids, orthothecimorphs, hyolithelminths, cap-shaped fossils, protoconodonts, and *Salanacus* are moved up to just below the positive $\delta^{13}C$ peak 3p. We demonstrate that with the new data from Mongolia, there are still three pulses of fossil first appearances. We suggest that the pulsed nature of these first appearances is largely the result of surges in regional sedimentation and limited phosphatization windows in the sections in Mongolia, China, and Siberia rather than global evolutionary tempos. Rates of global origination and diversification during this evolutionarily critical transition remains an important problem for paleontologists and geologists, and future global correlations should include confidence intervals that take into account regional and local sampling biases.

With integrated sequence stratigraphy and high-resolution $\delta^{13}C$ chemostratigraphy, we show that the large $\delta^{13}C$ excursions and major sequence boundaries occur at roughly the same frequency in the Zavkhan terrane, providing potential stratigraphic evidence that the high-frequency carbon isotope excursions in the earliest Cambrian could have been modulated by global sea-level change and corresponding weathering and burial events. Using a refined age model, we estimate that the lag time between maximum flooding surfaces and positive $\delta^{13}C$ excursions is 200,000–500,000 yr. Combined, these data provide parameters and testable hypotheses that can be used to better constrain the relationships between biological and environmental change during this major transition in life.

ACKNOWLEDGMENTS

We would like to thank A. Bayasgalan, B. Altantsetseg, S. Oyungerel, D. Oyun, and S. Lkhagva-Ochir for logistical assistance in Mongolia. We would like to thank our field assistants G. Sarantuya, J. Chuluunbaatar, M. Delger, M. Jugder, A. Dorj, O. Dandar, U. Khuchitbaatar, A. Rooney, D. Bradley, S. Moon, C. Dwyer, R. Anderson, and E. Smith for the tremendous help in the field and laboratory. We thank J. Creveling and D. Jones for insightful comments and help with some of the initial field work. We thank S. Porter, M. Zhu, E. Sperling, and A. Maloof for detailed and thoughtful reviews. We thank C. Bucholz for useful discussions. We thank S. Manley and G. Eischeid for the use of and assistance in laboratories at Harvard University. We thank National Aeronautics and Space Administration (NASA) Massachusetts Institute of Technology (MIT) Astrobiology node, NASA Geobiology grant NNH10ZDA001N-EXO, and National Science Foundation Graduate Research Fellowship Program to E. Smith for financial support.

REFERENCES CITED

Babcock, L.E., Robison, R.A., and Shanchi, P., 2011, Cambrian stage and series nomenclature of Laurentia and the developing global chronostratigraphic scale: Museum of Northern Arizona Bulletin, v. 67, p. 12–26.

Babcock, L.E., Peng, S., Zhu, M., Xiao, S., and Ahlberg, P., 2014, Proposed reassessment of the Cambrian GSSP: Journal of African Earth Sciences, v. 98, p. 3–10.

Baode, G., Ruitang, W., Hambrey, M. and Wuchen, G., 1986, Glacial sediments and erosional pavements near the Cambrian—Precambrian boundary in western Henan Province, China: Journal of the Geological Society, v. 143, no. 2, p. 311–323.

Bezzubtsev, V.V., 1963, On the Precambrian-Cambrian stratigraphy of the Dzabkhan River Basin, *in* Materials on the Geology of MPR: Gostopotekhizdat, p. 29–42.

Bold, U., Macdonald, F.A., Smith, E.F., Crowley, J.L., and Minjin, C., 2013, Elevating the Neoproterozoic Tsagaan-Olom Formation to a group: Mongolian Geoscientist, v. 39, no. 5, p. 89–94.

Bowring, S.A., Grotzinger, J.P., Condon, D.J., Ramezani, J., Newall, M.J., and Allen, P.A., 2007, Geochronologic constraints on the chronostratigraphic framework of the Neoproterozoic Huqf Supergroup, Sultanate of Oman: American Journal of Science, v. 307, no. 10, p. 1097–1145.

Brasier, M., and Lindsay, J.F., 2001, Did supercontinental amalgamation trigger the "Cambrian explosion," *in* Zhuravlev, A.Yu., and Riding, R., eds., The Ecology of the Cambrian Radiation: New York, Columbia University Press, p. 69–89.

Brasier, M., Magaritz, M., Corfield, R., Huilin, L., Xiche, W., Lin, O., Zhiwen, J., Hamdi, B., Tinggui, H., and Fraser, A., 1990, The carbon-and oxygen-isotope record of the Precambrian-Cambrian boundary interval in China and Iran and their correlation: Geological Magazine, v. 127, no. 4, p. 319–332.

Brasier, M., Khomentovsky, V., and Corfield, R., 1993, Stable isotopic calibration of the earliest skeletal fossil assemblages in eastern Siberia (Precambrian-Cambrian boundary): Terra Nova, v. 5, no. 3, p. 225–232.

Brasier, M., Dorjnamjaa, D., and Lindsay, J., 1996a, The Neoproterozoic to early Cambrian in southwest Mongolia: An introduction: Geological Magazine, v. 133, no. 4, p. 365–369.

Brasier, M., Shields, G., Kuleshov, V., and Zhegallo, E., 1996b, Integrated chemo- and biostratigraphic calibration of early animal evolution: Neoproterozoic–early Cambrian of southwest Mongolia: Geological Magazine, v. 133, no. 4, p. 445–485.

Buatois, L.A., Almond, J., and Germs, G.J., 2013, Environmental tolerance and range offset of *Treptichnus pedum*: Implications for the recognition of the Ediacaran-Cambrian boundary: Geology, v. 41, no. 4, p. 519–522.

Bucholz, C.E., Jagoutz, O., Schmidt, M.W., and Sambuu, O., 2014, Phlogopite- and clinopyroxene-dominated fractional crystallization of an alkaline primitive melt: Petrology and mineral chemistry of the Dariv igneous complex, western Mongolia: Contributions to Mineralogy and Petrology, v. 167, no. 4, p. 1–28.

Calver, C., Crowley, J., Wingate, M., Evans, D., Raub, T., and Schmitz, M., 2013, Globally synchronous Marinoan deglaciation indicated by U-Pb geochronology of the Cottons Breccia, Tasmania, Australia: Geology, v. 41, no. 10, p. 1127–1130.

Calver, C.R., Black, L.P., Everard, J.L., and Seymour, D.B., 2004, U-Pb zircon age constraints on late Neoproterozoic glaciation in Tasmania: Geology, v. 32, no. 10, p. 893–896.

Chumakov, N., and Elston, D., 1989, The paradox of Late Proterozoic glaciations at low latitudes: Episodes, v. 12, no. 2, p. 115.

Chumakov, N.M., 2011a, Glacial deposits of the Baykonur Formation, Kazakhstan and Kyrgyzstan: Geological Society, London, Memoirs, v. 36, no. 1, p. 303–307.

Chumakov, N.M., 2011b, Glacial deposits of the Bokson Group, East Sayan Mountains, Buryatian Republic, Russian Federation: Geological Society, London, Memoirs, v. 36, no. 1, p. 285–288.

Compston, W., Williams, I.S., Kirschvink, J.L., Zhang Zichao, and Ma Guogan, 1992, Zircon U-Pb ages from the Early Cambrian time-scale: Journal of the Geological Society of London, v. 149, p. 171–184, doi:10.1144/gsjgs.149.2.0171.

Condon, D., Zhu, M.Y., Bowring, S., Wang, W., Yang, A.H., and Jin, Y.G., 2005, U-Pb ages from the Neoproterozoic Doushantuo Formation, China: Science, v. 308, no. 5718, p. 95–98.

Corsetti, F.A., and Hagadorn, J.W., 2000, Precambrian-Cambrian transition: Death Valley, United States: Geology, v. 28, no. 4, p. 299–302.

Crimes, P.T., 1987, Trace fossils and correlation of late Precambrian and early Cambrian strata: Geological Magazine, v. 124, no. 2, p. 97–119.

Crimes, T.P., 1992, The record of trace fossils across the Proterozoic-Cambrian boundary, *in* Lipps, J.H., and Signor, P.W., eds., Origin and Early Evolution of the Metazoa: New York, Plenum Press, p. 177–202.

Darwin, C.R., 1859, On the Origin of Species by Means of Natural Selection, or the Preservation of Favoured Races in the Struggle for Life: London, Murray, 502 p.

Derry, L., Brasier, M., Corfield, R.A., Rozanov, A.Y., and Zhuravlev, A.Y., 1994, Sr and C isotopes in Lower Cambrian carbonates from the Siberian craton: A paleoenvironmental record during the 'Cambrian explosion': Earth and Planetary Science Letters, v. 128, no. 3, p. 671–681.

Dorjnamjaa, D., and Bat-Ireedui, Y., 1991, The Precambrian of Mongolia: Ulaanbaatar, Geological Institute of the Mongolian Academy of Sciences.

Dorjnamjaa, D., Bat-Ireedui, Y.A., Dashdavaa, Z., and Soelmaa, D., 1993, Precambrian-Cambrian Geology of the Dzavkhan Zone: Oxford, UK, Earth Sciences Department, University of Oxford, 36 p.

Edel, J.B., Schulmann, K., Hanžl, P., and Lexa, O., 2014, Palaeomagnetic and structural constraints on 90° anticlockwise rotation in SW Mongolia during the Permo–Triassic: Implications for Altaid oroclinal bending. Preliminary palaeomagnetic results: Journal of Asian Earth Sciences, v. 94, p. 157–171.

Endonzhamts, Zh., and Lkhasuren, B., 1988, Stratigrafi ya pogranichnykh tolshch dokembriya i kembriya Dzabkhanskoy zony, *in* Khomentovsky, V.V., and Shenfi l', V.Yu., eds., Pozdniy dokembriy i ranniy paleozoy Sibiri , Rifey i vend: Novosibirsk, Institut Geologii i Geofi ziki, Sibirskoe Otdelenie, Akademiya Nauk: SSSR, p. 150–162.

Erwin, D.H., Laflamme, M., Tweedt, S.M., Sperling, E.A., Pisani, D., and Peterson, K.J., 2011, The Cambrian conundrum: Early divergence and later ecological success in the early history of animals: Science, v. 334, no. 6059, p. 1091–1097.

Esakova, N.V., and Zhegallo, E.A., 1996, Stratigrafaya i fauna nizhnego Kembriya Mongolii (Lower Cambrian stratigraphy and fauna of Mongolia): Sovmestnaya Sovetsko-Mongol'skaya Paleontologicheskaya Ekspeditsiya, v. 46, p. 208.

Etemad-Saeed, N., Hosseini-Barzi, M., Adabi, M.H., Miller, N.R., Sadeghi, A., Houshmandzadeh, A., and Stockli, D.F., 2015, Evidence for ca. 560 Ma Ediacaran glaciation in the Kahar Formation, central Alborz Mountains, northern Iran: Gondwana Research (in press).

Gehling, J.G., Jensen, S., Droser, M.L., Myrow, P.M., and Narbonne, G.M., 2001, Burrowing below the basal Cambrian GSSP, Fortune Head, Newfoundland: Geological Magazine, v. 138, no. 2, p. 213–218.

Geyer, G., 2005, The Fish River Subgroup in Namibia: Stratigraphy, depositional environments and the Proterozoic-Cambrian boundary problem revisited: Geological Magazine, v. 142, no. 5, p. 465–498.

Geyer, G., and Uchman, A., 1995, Ichnofossil assemblages from the Nama Group (Neoproterozoic–Lower Cambrian) in Namibia and the Proterozoic-Cambrian boundary problem revisited: Beringeria, v. 2, Special Issue, p. 175–202.

Gibsher, A., and Khomentovsky, V., 1990, The section of the Tsagaan Oloom and Bayan Gol Formations of the Vendian–Lower Cambrian in the Dzabkhan zone of Mongolia, *in* The Late Precambrian and Early Paleozoic of Siberia: Novosibirsk, Institut Geologii i Geofiziki, Sibirskoe Otdelenie, Akademiya Nauk SSSR, p. 79–91.

Gibsher, A.S., Bat-Ireedui, Y.A., Balakhonov, I.G., and Efremenko, D.E., 1991, The Bayan Gol reference section of the Vendian–Lower Cambrian in central Mongolia, *in* Khomentovsky, V.V., ed., Late Precambrian and Early Palaeozoic of Siberia. Siberian Platform and its Framework: Novosibirsk, Ob'edinennyy Institut Geologii, Geofiziki i Mineralogii, Sibierskoe Otdelenie, Akademiya Nauk SSSR, p. 151.

Gibson, T., Myrow, P., Macdonald, F., Minjin, C., and Gehrels, G., 2013, Depositional history, tectonics, and detrital zircon geochronology of Ordovician and Devonian strata in southwestern Mongolia: Geological Society of America Bulletin, v. 125, no. 5–6, p. 877–893.

Goldring, R., and Jensen, S., 1996, Trace fossils and biofabrics at the Precambrian-Cambrian boundary interval in western Mongolia: Geological Magazine, v. 133, no. 4, p. 403–415.

Grotzinger, J.P., Bowring, S.A., Saylor, B.Z., and Kaufman, A.J., 1995, Biostratigraphic and geochronologic constraints on early animal evolution: Science, v. 270, no. 5236, p. 598–604.

He, T., Shen, L., and Yan, J., 1988, A new understanding on Meishucun Sinian-Cambrian boundary section in Jinning: Yunnan Journal of Chengdu University of Technology (Science & Technology Edition), v. 3, p. 5.

Hebert, C.L., Kaufman, A.J., Penniston-Dorland, S.C., and Martin, A.J., 2010, Radiometric and stratigraphic constraints on terminal Ediacaran (post-Gaskiers) glaciation and metazoan evolution: Precambrian Research, v. 182, no. 4, p. 402–412.

Hoffman, P., 1967, Algal stromatolites: Use in stratigraphic correlation and paleocurrent determination: Science, v. 157, no. 3792, p. 1043–1045.

Jahn, B.-M., Litvinovsky, B., Zanvilevich, A., and Reichow, M., 2009, Peralkaline granitoid magmatism in the Mongolian–Transbaikalian belt: Evolution, petrogenesis and tectonic significance: Lithos, v. 113, no. 3, p. 521–539.

Johnston, D., Macdonald, F., Gill, B., Hoffman, P., and Schrag, D., 2012, Uncovering the Neoproterozoic carbon cycle: Nature, v. 483, no. 7389, p. 320–323.

Kaufman, A.J., Knoll, A.H., Semikhatov, M.A., Grotzinger, J.P., Jacobsen, S.B., and Adams, W., 1996, Integrated chronostratigraphy of Proterozoic-Cambrian boundary beds in the western Anabar region, northern Siberia: Geological Magazine, v. 133, no. 5, p. 509–533.

Khomentovsky, V., and Gibsher, A., 1996, The Neoproterozoic–Lower Cambrian in northern Govi-Altay, western Mongolia: Regional setting, lithostratigraphy and biostratigraphy: Geological Magazine, v. 133, no. 04, p. 371–390.

Khomentovsky, V., and Karlova, G., 1993, Biostratigraphy of the Vendian-Cambrian beds and the Lower Cambrian boundary in Siberia: Geological Magazine, v. 130, no. 1, p. 29–45.

Kirschvink, J., and Raub, T., 2003, A methane fuse for the Cambrian explosion: True polar wander: Comptes Rendus Geoscience, v. 335, p. 71–83.

Kirschvink, J.L., Magaritz, M., Ripperdan, R.L., Zhuravlev, A.Y., and Rozanov, A.Y., 1991, The Precambrian-Cambrian boundary: Magnetostratigraphy and carbon isotopes resolve correlation problems between Siberia, Morocco, and South China: GSA Today, v. 1, no. 4, p. 69–91.

Knoll, A.H., Grotzinger, J.P., Kaufman, A.J., and Kolosov, P., 1995a, Integrated approaches to terminal Proterozoic stratigraphy: An example from the Olenek Uplift, northeastern Siberia: Precambrian Research, v. 73, no. 1, p. 251–270.

Knoll, A.H., Kaufman, A.J., Semikhatov, M.A., Grotzinger, J.P., and Adams, W., 1995b, Sizing up the sub-Tommotian unconformity in Siberia: Geology, v. 23, no. 12, p. 1139–1143.

Korobov, M., and Missarzhevsky, V., 1977, O pogranichnykh sloyakh kembriya i dokembriya Zapadnoy Mongolii (khrebet Khasagt-Khairkhan): Bespozvonochnye paleozoya Mongolii: Sovmestnaya Sovestsko-Mongol'skaya Paleontologicheskaya Ekspeditsiya: Trudy, v. 5, p. 7–9.

Kouchinsky, A., Bengtson, S., Missarzhevsky, V.V., Pelechaty, S., Torssander, P., and Val'kov, A.K., 2001, Carbon isotope stratigraphy and the problem of a pre–Tommotian Stage in Siberia: Geological Magazine, v. 138, no. 4, p. 387–396.

Kouchinsky, A., Bengtson, S., Pavlov, V., Runnegar, B., Torssander, P., Young, E., and Ziegler, K., 2007, Carbon isotope stratigraphy of the Precambrian–Cambrian Sukharikha River section, northwestern Siberian platform: Geological Magazine, v. 144, no. 4, p. 609–618.

Kröner, A., Lehmann, J., Schulmann, K., Demoux, A., Lexa, O., Tomurhuu, D., Štípská, P., Liu, D., and Wingate,

M.T., 2010, Lithostratigraphic and geochronological constraints on the evolution of the Central Asian orogenic belt in SW Mongolia: Early Paleozoic rifting followed by late Paleozoic accretion: American Journal of Science, v. 310, no. 7, p. 523–574.

Kruse, P.D., Gandin, A., Debrenne, F., and Wood, R., 1996, Early Cambrian bioconstructions in the Zavkhan Basin of western Mongolia: Geological Magazine, v. 133, no. 4, p. 429–444.

Landing, E., 1988, Lower Cambrian of eastern Massachusetts: Stratigraphy and small shelly fossils: Journal of Paleontology, v. 62, p. 661–695.

Landing, E., 1994, Precambrian-Cambrian boundary global stratotype ratified and a new perspective of Cambrian time: Geology, v. 22, no. 2, p. 179–182.

Landing, E., Geyer, G., Brasier, M.D., and Bowring, S.A., 2013, Cambrian evolutionary radiation: Context, correlation, and chronostratigraphy—Overcoming deficiencies of the first appearance datum (FAD) concept: Earth-Science Reviews, v. 123, p. 133–172.

Lehmann, J., Schulmann, K., Lexa, O., Corsini, M., Kroner, A., Stipska, P., Tomurhuu, D., and Otgonbator, D., 2010, Structural constraints on the evolution of the Central Asian orogenic belt in SW Mongolia: American Journal of Science, v. 310, no. 7, p. 575–628.

Levashova, N.M., Kalugin, V.M., Gibsher, A.S., Yff, J., Ryabinin, A.B., Meert, J., and Malone, S.J., 2010, The origin of the Baydaric microcontinent, Mongolia: Constraints from paleomagnetism and geochronology: Tectonophysics, v. 485, no. 1–4, p. 306–320.

Li, D., Ling, H.-F., Jiang, S.-Y., Pan, J.-Y., Chen, Y.-Q., Cai, Y.-F., and Feng, H.-Z., 2009, New carbon isotope stratigraphy of the Ediacaran-Cambrian boundary interval from SW China: Implications for global correlation: Geological Magazine, v. 146, no. 4, p. 465–484.

Li, G., Zhao, X., Gubanov, A., Zhu, M., and Na, L., 2011, Early Cambrian mollusc *Watsonella crosbyi*: A potential GSSP index fossil for the base of the Cambrian Stage 2: Acta Geologica Sinica, v. 85, no. 2, p. 309–319 [English edition].

Lindsay, J., Brasier, M., Dorjnamjaa, D., Goldring, R., Kruse, P., and Wood, R., 1996a, Facies and sequence controls on the appearance of the Cambrian biota in southwestern Mongolia: Implications for the Precambrian-Cambrian boundary: Geological Magazine, v. 133, no. 4, p. 417–428.

Lindsay, J., Brasier, M., Shields, G., Khomentovsky, V., and Bat-Ireedui, Y., 1996b, Glacial facies associations in a Neoproterozoic back-arc setting, Zavkhan Basin, western Mongolia: Geological Magazine, v. 133, no. 4, p. 391–402.

Macdonald, F.A., 2011, The Tsagaan Oloom Formation, southwestern Mongolia, *in* Arnaud, E., Halverson, G.P., and Shields-Zhou, G., eds., The Geological Record of Neoproterozoic Glaciations: Geological Society of London Memoir 36, p. 331–337.

Macdonald, F.A., Jones, D.S., and Schrag, D.P., 2009, Stratigraphic and tectonic implications of a new glacial diamictite–cap carbonate couplet in southwestern Mongolia: Geology, v. 37, p. 123–126.

Macdonald, F.A., Schmitz, M.D., Crowley, J.L., Roots, C.F., Jones, D.S., Maloof, A.C., Strauss, J.V., Cohen, P.A., Johnston, D.T., and Schrag, D.P., 2010, Calibrating the Cryogenian: Science, v. 327, no. 5970, p. 1241–1243.

MacNaughton, R.B., and Narbonne, G.M., 1999, Evolution and ecology of Neoproterozoic–Lower Cambrian trace fossils, NW Canada: Palaios, v. 14 p. 97–115.

Maloof, A.C., Schrag, D.P., Crowley, J.L., and Bowring, S.A., 2005, An expanded record of early Cambrian carbon cycling from the Anti-Atlas Margin, Morocco: Canadian Journal of Earth Sciences, v. 42, no. 12, p. 2195–2216.

Maloof, A.C., Porter, S.M., Moore, J.L., Dudás, F.Ö., Bowring, S.A., Higgins, J.A., Fike, D.A., and Eddy, M.P., 2010a, The earliest Cambrian record of animals and ocean geochemical change: Geological Society of America Bulletin, v. 122, no. 11–12, p. 1731–1774.

Maloof, A.C., Ramezani, J., Bowring, S.A., Fike, D.A., Porter, S.M., and Mazouad, M., 2010b, Constraints on early Cambrian carbon cycling from the duration of the Nemakit-Daldynian–Tommotian boundary $\delta^{13}C$ shift, Morocco: Geology, v. 38, no. 7, p. 623–626.

Markova, N., Korobov, M., and Zhuravleva, Z., 1972, K voprosu o vend-kembriyskikh otlozheniyakh Yugo-Zapadnoy Mongolii (On the problem of the Vendian-Cambrian deposits of southwestern Mongolia): Bulleten'Moskovskogo Obshchestva Ispytateley Prirody, Otdel Geologicheskiy, v. 47, no. 1, p. 57–70.

Marshall, C.R., 2006, Explaining the Cambrian "explosion" of animals: Annual Review of Earth and Planetary Sciences, v. 34, p. 355–384.

Meert, J.G., and Van der Voo, R., 1994, The Neoproterozoic (1000–540 Ma) glacial intervals: No more snowball Earth?: Earth and Planetary Science Letters, v. 123, no. 1, p. 1–13.

Mullins, H.T., Gardulski, A.F., Wise, S.W., and Applegate, J., 1987, Middle Miocene oceanographic event in the eastern Gulf of Mexico: Implications for seismic stratigraphic succession and Loop Current/Gulf Stream circulation: Geological Society of America Bulletin, v. 98, no. 6, p. 702–713.

Narbonne, G.M., Kaufman, A.J., and Knoll, A.H., 1994, Integrated chemostratigraphy and biostratigraphy of the Windermere Supergroup, northwestern Canada: Implications for Neoproterozoic correlations and the early evolution of animals: Geological Society of America Bulletin, v. 106, no. 10, p. 1281–1292.

Parkhaev, P.Y., 2007, Shell chirality in Cambrian gastropods and sinistral members of the genus *Aldanella Vostokova*, 1962: Paleontological Journal, v. 41, no. 3, p. 233–240.

Parkhaev, P.Y., Karlova, G., and Rozanov, A.Y., 2011, Taxonomy, stratigraphy and biogeography of *Aldanella attleborensis*—A possible candidate for defining the base of Cambrian Stage 2: Museum of Northern Arizona Bulletin, v. 67, p. 298–300.

Peng, S., Babcock, L., and Cooper, R., 2012, The Cambrian Period, *in* Gradstein, J.G., Ogg, M., Schmitz, and Ogg, G., eds., The Geologic Time Scale, Volume 2: Cambridge, UK, Cambridge University Press, p. 437–488.

Porter, S.M., 2004, Closing the phosphatization window: Testing for the influence of taphonomic megabias on the pattern of small shelly fossil decline: Palaios, v. 19, no. 2, p. 178–183.

Porter, S.M., 2007, Seawater chemistry and early carbonate biomineralization: Science, v. 316, no. 5829, p. 1302.

Qian, Y., and Bengtson, S., 1989, Palaeontology and biostratigraphy of the Early Cambrian Meishucunian Stage in Yunnan Province, South China: Oslo, Norway, Universitetsforlaget, 156 p.

Qian, Y., Zhu, M., He, T., and Jiang, Z., 1996, New investigation of Precambrian-Cambrian boundary sections in eastern Yunnan: Acta Micropalaontologica Sinica, v. 13, p. 225–240.

Repina, L., and Rozanov, A., 1992, The Cambrian of Siberia: Novosibirsk: Trudy Instituta Geologii Geofi ziki, v. 788, p. 135.

Rice, A.H.N., Edwards, M.B., Hansen, T.A., Arnaud, E., and Halverson, G.P., 2011, Glaciogenic rocks of the Neoproterozoic Smalfjord and Mortensnes formations, Vestertana Group, E. Finnmark, Norway: Geological Society, London, Memoirs, v. 36, no. 1, p. 593–602.

Rooney, A.D., Macdonald, F.A., Strauss, J.V., Dudás, F.Ö., Hallmann, C., and Selby, D., 2014, Re-Os geochronology and coupled Os-Sr isotope constraints on the Sturtian snowball Earth: Proceedings of the National Academy of Sciences of the United States of America, v. 111, no. 1, p. 51–56.

Rozanov, A.Y., Khomentovsky, V., Shabanov, Y.Y., Karlova, G., Varlamov, A., Luchinina, V., Demidenko, Y.E., Parkhaev, P.Y., Korovnikov, I., and Skorlotova, N., 2008, To the problem of stage subdivision of the Lower Cambrian: Stratigraphy and Geological Correlation, v. 16, no. 1, p. 1–19.

Ruzhentsev, S.V., and Burashnikov, V.V., 1996, Tectonics of the western Mongolian Salairides: Geotectonics, v. 29, no. 5, p. 379–394.

Schrag, D.P., Higgins, J.A., Macdonald, F.A., and Johnston, D.T., 2013, Authigenic carbonate and the history of the global carbon cycle: Science, v. 339, no. 6119, p. 540–543.

Schröder, S., and Grotzinger, J., 2007, Evidence for anoxia at the Ediacaran-Cambrian boundary: The record of redox-sensitive trace elements and rare earth elements in Oman: Journal of the Geological Society of London, v. 164, no. 1, p. 175–187.

Shields, G.A., Brasier, M.D., Stille, P., and Dorjnamjaa, D.-I., 2002, Factors contributing to high $\delta^{13}C$ values in Cryogenian limestones of western Mongolia: Earth and Planetary Science Letters, v. 196, no. 3, p. 99–111.

Shields-Zhou, G., Hill, A., and Macgabhann, B., 2012, The Cryogenian Period, *in* Gradstein, J.G., Ogg, M., Schmitz, and Ogg, G., eds., The Geologic Time Scale: Cambridge, UK, Cambridge University Press, p. 393–411.

Spence, G.H., and Tucker, M.E., 1997, Genesis of limestone megabreccias and their significance in carbonate sequence stratigraphic models: A review: Sedimentary Geology, v. 112, no. 3, p. 163–193.

Squire, R.J., Campbell, I.H., Allen, C.M., and Wilson, C.J., 2006, Did the Transgondwanan Supermountain trigger the explosive radiation of animals on Earth?: Earth and Planetary Science Letters, v. 250, no. 1, p. 116–133.

Steiner, M., Li, G., Qian, Y., Zhu, M., and Erdtmann, B.-D., 2007, Neoproterozoic to early Cambrian small shelly fossil assemblages and a revised biostratigraphic correlation of the Yangtze Platform (China): Palaeogeography, Palaeoclimatology, Palaeoecology, v. 254, no. 1, p. 67–99.

Stodt, F., Rice, A.H.N., Björklund, L., Bax, G., Halverson, G.P., and Pharaoh, T., 2011, Evidence of late Neoproterozoic glaciation in the Caledonides of NW Scandinavia: Geological Society, London, Memoirs, v. 36, no. 1, p. 603–612.

Torsvik, T., Smethurst, M., Meert, J.G., Van der Voo, R., McKerrow, W., Brasier, M., Sturt, B., and Walderhaug, H., 1996, Continental break-up and collision in the Neoproterozoic and Palaeozoic—A tale of Baltica and Laurentia: Earth-Science Reviews, v. 40, no. 3, p. 229–258.

Vail, P.R., Mitchum Jr, R., and Thompson, S., III, 1977, Seismic stratigraphy and global changes of sea level: Part 4. Global cycles of relative changes of sea level. Section 2. Application of seismic reflection configuration to stratigraphic interpretation, *in* Payton, C.E., Seismic Stratigraphy—Applications to Hydrocarbon Exploration: American Association of Petroleum Geologists Memoir 26, p. 83–97.

Valentine, J.W., 2002, Prelude to the Cambrian explosion: Annual Review of Earth and Planetary Sciences, v. 30, no. 1, p. 285–306.

Van Wagoner, J.C., Mitchum, R., Campion, K., and Rahmanian, V., 1990, Siliciclastic Sequence Stratigraphy in Well Logs, Cores, and Outcrops: Concepts for High-Resolution Correlation of Time and Facies: American Association of Petroleum Geologists Methods 7, 55 p.

Voronin, Y.I., Voronova, L.G., Girgor'eva, N.V., Drozdova, N.A., Zhegallo, E.A., Zhuravlev, A.Y., Ragozina, A.L., Rozanov, A.Y., Sayutina, T.A., Sysoev, V.A., and Fonin, V.D., 1982, The Precambrian/Cambrian boundary in the geosynclinal areas (the reference section of Salaany-Gol, MPR): Moscow, Akademia Nauk SSSR, Trudy Sovmestnoy Sovetsoko-Mongol'skoy Paleontologicheskoy Ekspeditsii, 150 p.

Wilhem, C., Windley, B.F., and Stampfli, G.M., 2012, The Altaids of Central Asia: A tectonic and evolutionary innovative review: Earth-Science Reviews, v. 113, no. 3, p. 303–341.

Wille, M., Nägler, T.F., Lehmann, B., Schröder, S., and Kramers, J.D., 2008, Hydrogen sulphide release to surface waters at the Precambrian/Cambrian boundary: Nature, v. 453, no. 7196, p. 767–769.

Wood, R., Zhuravlev, A.Y., and Anaaz, C.T., 1993, The ecology of Lower Cambrian buildups from Zuune Arts, Mongolia: Implications for early metazoan reef evolution: Sedimentology, v. 40, no. 5, p. 829–858.

Yang, B., Steiner, M., Li, G., and Keupp, H., 2014, Terreneuvian small shelly faunas of East Yunnan (South China) and their biostratigraphic implications: Palaeogeography, Palaeoclimatology, Palaeoecology, v. 398, p. 28–58.

Yarmolyuk, V., Kovalenko, V., Anisimova, I., Sal'nikova, E., Kovach, V., Kozakov, I., Kozlovsky, A., Kudryashova, E., Kotov, A., and Plotkina, Y.V., Late Riphean

alkali granites of the Zabhan microcontinent: Evidence for the timing of Rodinia breakup and formation of microcontinents in the Central Asian fold belt, *in* Proceedings Doklady Earth Sciences 2008, Volume 420: Springer, p. 583–588.

Zhegallo, L., and Zhuravlev, A.Y., 1991, Guidebook for the International Excursion to the Vendian-Cambrian Deposits of the Dzvkhan Zone of Mongolia: Moscow, Palaeontological Institute, 24 p.

Zhou, C., Zhang, J., Li, G., and Yu, Z., 1997, Carbon and oxygen isotopic record of the early Cambrian from the Xiaotan Section, Yunnan, South China: Scientia Geologica Sinica, v. 32, no. 2, p. 201–211.

Zhu, M., and Wang, H., 2011, Neoproterozoic glaciogenic diamictites of the Tarim Block, NW China: Geological Society, London, Memoirs, v. 36, no. 1, p. 367–378.

Zhu, M., Li, G., Zhang, J., and Michael, S., 2001, Early Cambrian stratigraphy of east Yunnan, southwestern China: A synthesis, *in* Zhu, M., Van Iten, H., Peng, S., and Li, G., eds., The Cambrian of South China: Acta Palaeontologica Sinica, v. 40, p. 4–39.

Zhu, M., Strauss, H., and Shields, G.A., 2007, From snowball Earth to the Cambrian bioradiation: Calibration of Ediacaran–Cambrian Earth history in South China: Palaeogeography, Palaeoclimatology, Palaeoecology, v. 254, no. 1, p. 1–6.

Zhu, M.-Y., Babcock, L.E., and Peng, S.-C., 2006, Advances in Cambrian stratigraphy and paleontology: Integrating correlation techniques, paleobiology, taphonomy and paleoenvironmental reconstruction: Palaeoworld, v. 15, no. 3, p. 217–222.

Science Editor: Christian Koeberl
Associate Editor: Kenneth G. MacLeod

Manuscript Received 8 December 2014
Revised Manuscript Received 4 May 2015
Manuscript Accepted 8 July 2015

Printed in the USA

THE GEOLOGICAL SOCIETY OF AMERICA®

Errata

Integrated stratigraphic, geochemical, and paleontological late Ediacaran to early Cambrian records from southwestern Mongolia
Emily F. Smith, Francis A. Macdonald, Tanya A. Petach, Uyanga Bold, and Daniel P. Schrag
(v. 128; no. 3/4; p. 442–468; doi: 10.1130/B31248.1)

The captions for Figures 7 and 9 were switched. Following are the correct captions:

Figure 7. (A) Autochthonous to allochthonous thrust sheets of different facies of the Khairkhan Formation and cumulate ultramafics and serpentinite. Clasts of ultramafic rock have been found in the Khairkhan Formation. Together, these stratigraphic and sedimentological results support the claim that the Zavkhan Basin was a foreland basin (Macdonald et al., 2009). (B) Photo of the cumulative ultramafics in thrust contact with the Salaagol Formation in northern Orolgo Gorge. (C) Photo of the parautochthonous facies of the Khairkhan Formation from SE Khukh-Davaa area.

Figure 9. Integrated lithostratigraphy, sequence stratigraphy, and $\delta^{13}C$ chemostratigraphy of the Zuun-Arts and Bayangol Formations. Measured sections are numbered according to proximity to the paleoshoreline, with more distal sections on the right and more proximal sections on the left. Locations of the individual measured sections are shown on the map in the lower-left side of the figure. Small shelly fossils (SSFs) horizons from this study are marked with red stars, and those from previous studies are marked with green stars. Purple circles mark ichnofossil horizons. Previous paleontological data from Orolgo (Orolchayn) Gorge is revised from Endonzhamts and Lkhasuren (1988). Paleontological data from Salaa and Tsagaan Gorges are from Voronin et al. (1982), Esakova and Zhegallo (1996), and Khomentovsky and Gibsher (1996). The paleontological data from Bayan Gorge are from Khomentovsky and Gibsher (1996). Each of the previous small shelly fossil horizons is labeled according to the labeling schemes of the different collections. Shaded colored boxes show correlation between sections. VPDB—Vienna Peedee belemnite; HST—highstand systems tract; TST—transgressive systems tract; LST—lowstand systems tract.

Low seasonality in central equatorial Pangea during a late Carboniferous highstand based on high-resolution isotopic records of brachiopod shells
Andy Roark, Ethan L. Grossman, and Joseph Lebold
(v. 128; no. 3/4; p. 597–608; doi: 10.1130/B31330.1)

The right axis label is incorrect in Figure 5B. Please see the corrected figure here.